1-1-2016

Kinematic molecular manufacturing machines

Danijel Boskovic
University of Wollongong, db103@uowmail.edu.au

Sivakumar Balakrishnan
University of Wollongong

Shaoming Huang
Wenzhou University

Gerhard F. Swiegers
University of Wollongong, swiegers@uow.edu.au

Kinematic molecular manufacturing machines

Abstract

The principles of kinematic manufacturing machines of the type widely used since the industrial revolution are reviewed. Consideration is then given to how the principles of kinematics ('the geometry of motion') may manifest in molecular catalysts. Actions of this type involve synchronized, regular, repeated and rapid conformational flexing along geometrically optimum pathways that define a single degree of freedom. The proposition that many of the catalysts of biology, enzymes, may generally exploit a kinematic action is discussed. Thereafter, in the major portion of this work, representative abiological molecular catalysts whose actions display the characteristic features of kinematic manufacturing processes, are reviewed. In accordance with the principles of kinematics, molecular catalytic actions of this type are shown to be capable of transforming unremarkable chemical species into powerful catalysts with high activities, selectivities, and durabilities.

Disciplines

Engineering | Physical Sciences and Mathematics

Publication Details

Boskovic, D., Balakrishnan, S., Huang, S. & Swiegers, G. F. (2016). Kinematic molecular manufacturing machines. Coordination Chemistry Reviews, 329 163-190.

Kinematic Molecular Manufacturing Machines

Danijel Boskovic,[a] Sivakumar Balakrishnan,[a] Shaoming Huang,[b] and Gerhard F. Swiegers[a,b]*

[a] Intelligent Polymer Research Institute (IPRI) and the ARC Centre of Excellence for Electromaterials Science (ACES), University of Wollongong, Wollongong, NSW 2522, Australia; E-mail: swiegers@uow.edu.au

[b] Zhejiang Key Laboratory of Carbon Materials, College of Chemistry and Material Engineering, Wenzhou University, Wenzhou 325027, Peoples Republic of China

Abstract: The principles of kinematic manufacturing machines of the type widely used since the industrial revolution are reviewed. Consideration is then given to how the principles of kinematics ('the geometry of motion') may manifest in molecular catalysts. Actions of this type involve synchronized, regular, repeated and rapid conformational flexing along geometrically optimum pathways that define a single degree of freedom. The proposition that many of the catalysts of biology, enzymes, may generally exploit a kinematic action is discussed. Thereafter, in the major portion of this work, representative abiological molecular catalysts whose actions display the characteristic features of kinematic manufacturing processes, are reviewed. In accordance with the principles of kinematics, molecular catalytic actions of this type are shown to be capable of transforming unremarkable chemical species into powerful catalysts with high activities, selectivities, and durabilities.

Dedicated to the memory of Professor R. J. P. ("Bob") Williams FRS

1. Introduction

Modern human society is totally dependent on efficient manufacturing machines for the rapid, high-volume production of goods. The traditional view of industrial manufacturing involves large-scale machines utilising carefully designed kinematics, to mass-produce items. The term "*kinematic*" is defined as the "*geometry of motion*" [1]. That is, industrial manufacturing typically involves machines that synchronously employ regular, repeated, rapid motion along geometrically optimized pathways, to fabricate products at high speed and in large volumes.

A recent trend has been toward the miniaturisation of machines. That trend leads to the molecular domain and, ultimately, to the development of kinematic manufacturing machines that operate at the molecular level. Richard Feynman first raised the concept of artificial molecular-scale manufacturing machines in his seminal 1959 talk "*There's Plenty of Room at the Bottom*" [2]. Feynman posited the idea of utilising nanotechnology to construct matter at the atomic scale and upwards. The concept revolved around a tiny robot the size of a nanoparticle that would physically attach atoms to one another, building up structures by design. While this concept has not, to date, been practically realized, it nonetheless expressed the historic shift from large and impressive technology (e.g. ships, bridges and skyscrapers) to small and efficient technology (e.g. microchips and robotics).

At nearly the same time, biology was entering the molecular scale with Linus Pauling's work (1948) on the function of proteins and later with Watson and Crick's discovery of DNA (1953) as the core mechanism of genetics and therefore life. The continued focus on molecular scale processes in biology has since led to the establishment of molecular biology

and modern biotechnology. In a similar vein to Feynman's proposal, biological enzymes have, for some time, been thought of and referred to as "*machine-like*" in their actions [3].

Expanding on that notion, various authors have considered the idea of kinematic molecular manufacturing machines comprising gears, cogs, and moving parts in the scale of 1-1000 nm [4,5]. Such devices would, in theory, be capable of transporting reagents to active sites and forming molecules from molecular or atomic substrates in a process described by one author as *"mechanosynthesis*" [5]. However, the concept of *nano-machines* comprising of ultra-small machined parts, has proven to be exceedingly difficult to realise, even with the availability of atomic fabrication and placement techniques. Moreover, molecular biology, has increasingly come to contemplate the proposition that many enzymes may already be "molecular manufacturing machines" by virtue of the fact that they appear to exploit many of the general principles of such machines (*vide infra*).

In this work we review the key properties of large-scale, industrial, kinematic manufacturing machines. We then examine how these properties have been, or are likely to be realised at the molecular scale in catalytic systems. While reference is made to the operation of selected enzymes or to enzymes generally as a class, the focus of this work is on reviewing *abiological* molecular catalysts that may be said to utilize some or all of the principles of kinematic manufacturing processes. The intention in this respect, is to define, clarify and systematize the fundamental principles of kinematic manufacturing at the molecular level. It is also to unearth and highlight abiological examples that open a path to a potentially new, promising, emergent field of the future.

While numerous reviews have examined "molecular machines" that facilitate transport, switching, signalling, or other aspects of machine behaviour [6], the concept of high speed, continuous, kinematic manufacturing at the molecular level has not, to the best of our knowledge, been considered or reviewed. The present work is intended to fill that gap. It is also intended to stimulate consideration as to how kinematic manufacturing processes may manifest themselves in molecular systems and whether the power of well-known but unusually active catalysts like enzymes, may, in fact, be based on the principles of such processes.

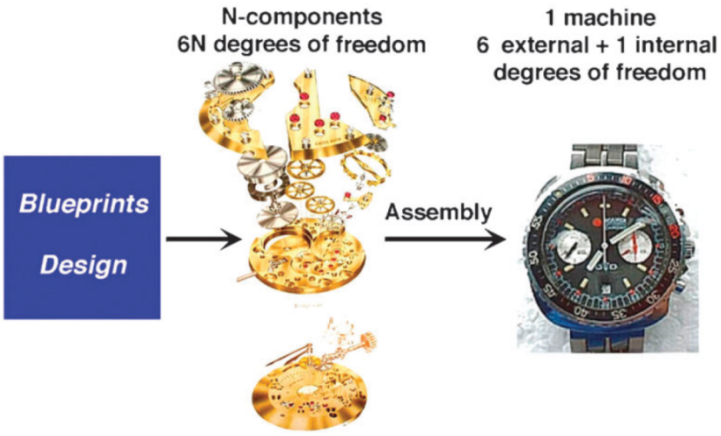

Figure 1. *Archetypal machine utilizing a 'kinematic' action – a wristwatch (Reproduced with permission from reference [7]).*

2. The Principles of Kinematic Manufacturing Machines

2.1 Examples of Kinematic Machines and Kinematic Manufacturing Machines

A machine is generally defined as a dense, multicomponent assembly of parts that transmits force, motion or energy from one component to another [7]. An example in this respect is a

wristwatch (Figure 1), which may be made up of, for example, 200 parts (N=200) that are designed to work collectively as one. While the separate parts have ca. 6N = 1200 independent degrees of freedom, they are assembled within the wristwatch in such a way that the entire assembly has only one internal degree of freedom. Its function is achieved by combining a large number of components within a structurally complex and dense assembly in such a way that each component is limited to a particular trajectory and/or dynamics.

Machines of this type operate due to a driving impulse, which is typically mechanical in character. In a wristwatch, for example, that impulse is provided by a wound spring that repeatedly and regularly alters the structure every one second. Machines of this type display a '*kinematic*'character. The term *kinematic* refers to the *"geometry of motion" [1],* by which the driving impulse is transmuted along very particular, well-defined, geometric pathways.

A kinematic manufacturing machine differs from a wristwatch in that the driving impulse is not simply utilized to repeatedly and regularly change the mechanical structure from one state to the next. Rather, it is harnessed to dynamically take up starting materials and mechanically transform them into new products. It does this by picking up and moving the starting materials on a very particular time-scale, through a well-defined and invariant set of geometric motions, constrained by the single degree of freedom that is available, until they are transformed into products. The products are then dynamically ejected. The cycle repeats itself regularly and rapidly, generating another product on each occassion. The rate of production that is achieved depends on the rapidity of the motion and the extent to which it is optimized.

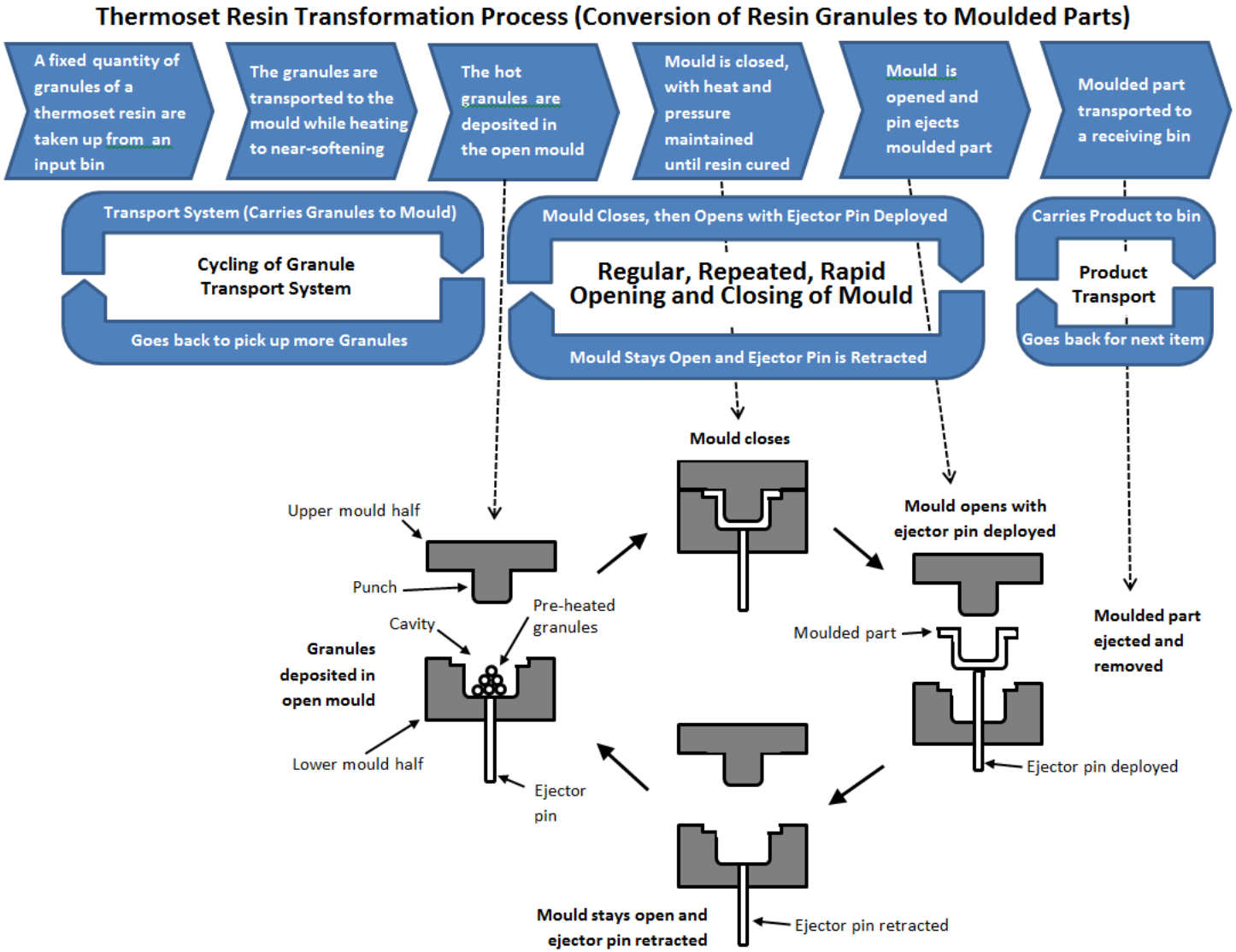

Figure 2. *Repetitive kinematic cycle in a typical compression moulding machine, showing three independent cycling processes that must be coupled to each other and synchronized in order for the machine to function properly. The processes are: (i) granule take-up, transport and deposition in the mould ('Granule Transport System'), (ii) the opening and closing of the mould, with deployment and retraction of the ejector pin, and (iii) product ejection and transport to the receiving bin ('Product Transport'). Each process operates independently but must be made to work synchronously with the other processes in order for the machine to function.*

An illustrative example of a kinematic manufacturing machine is a compression moulding machine, which converts granules of a thermoset resin into moulded parts. Figure 2 illustrates how such a machine works.

The upper-most blocks in Figure 2 comprise a "*Process Flow Diagram*" that shows the sequence of steps that the thermoset resin is taken through in its transformation, from granules at the start, to a moulded product at the end. The steps are depicted as the line of 'blocks' going across the very top of each figure, commencing with the starting materials (on the left) and ending with the final product (on the right).

Immediately below the Process Flow Diagram, in the centre of Figure 2, is shown the three independent cycling systems in compression moulding machines that operate in parallel and that sequentially interact with the thermoset resin. A schematic at the bottom of Figure 2 illustrates the operation of the central cycling system (the mould itself).

The left-most cycling system ('*Granule Transport System*') typically withdraws a carefully pre-determined number of granules from a storage container ('input bin') and transports them to the compression mould, heating them in transit. At a precise instant in time, the softened granules are deposited in the hot mould, which must be open and ready to accept the granules.

The opening and closing of the mould comprises the second, independent system in the machine, which is represented by the cycle shown at the centre in the middle of Figure 2 and having the cyclical steps illustrated schematically at the bottom of Figure 2. After deposition of the granules in the mould, the male and female parts of the mould are closed, with the

resulting heat and pressure causing the resin inside to cure. The mould is then opened, whereafter an ejector pin is deployed to eject the finished piece. Following retraction of the ejector pin, the open mould is ready to accept the next set of granules, in a regular (and, typically, rapid) repetition of the moulding process.

The moulded product that is formed is picked up and transported to a storage container ('receiving bin') by a third independent cycling system ('Product Transport System') depicted at the middle right of Figure 2.

The machine repeats the above processes cyclically, meaning that the three independent systems for (i) granule pick-up, transport, and deposition in the mould, (ii) mould opening and closing, and (iii) product ejection and transport away from the mould, must be coupled to each other and synchronized in order for the machine to function correctly. The term "*synchronized*" means that each process must interact with the next one in the sequence at a very particular, well-defined instant in time. That is, for example, the granule transport system must deposit granules into the mould *only* when the mould is at the correct stage of its cycle – that is, when the mould is open, empty, and with the ejector pin retracted. The product transport system should similarly only interact with the mould when the mould is open and the ejector pin has pushed out a moulded product.

Not only must the granule and product transport systems interact with the opening and closing cycle of the mould at very particular, precise instances in time, but they must also do so on *each and every* occasion that they are required to do so, without fail. If one of those systems does not interact with the opening and closing cycle of the mould on *even one occasion*, then the machine may become jammed and inoperable. That is, if there is even one

error during one cycle in the sequence shown in Figure 2, then it may result in a complete loss of functionality and not a mere degradation of functionality.

The productivity of the machine is therefore wholly dependent on the precision, synchronicity, and reliability with which it carries out each of the necessary steps in the process, as well as the overall speed of their motion. The more rapid, reliable, and precisely accurate the motion, the faster and more productive the machine will be. In the real world, compression moulding machines can achieve extraordinary "activities", with production rates in the order of 10 products s^{-1} (or >30,000 h^{-1}) not unusual.

2.2 Key Features of Kinematic Manufacturing Machines

This example illustrates some of the key features of kinematic manufacturing machines, which include the following:

(1) *Regular, repetitive, and often rapid cyclical motion* by:

(2) a multiplicity of *components* whose actions are *coupled* under the influence of:

(3) a *mechanical (kinematic) impetus*, where the motions are cumulatively:

(4) restricted to *a single, geometrically-defined degree of freedom* that constitutes the manufacturing action, and where:

(5) the manufacturing site *interacts dynamically and rapidly* to take up starting materials and eject the products that are generated.

In order to optimally couple to each other, the parts of a kinematic manufacturing machine must typically be precisely designed and machined so as to *structurally complement* the other

parts with which they interact. Thus, for example, the use of interdigitating cogs that are structurally complementary to each other, is commonplace in kinematic manufacturing machines. Parts of the machine may also structurally complement the starting materials (during dynamic take-up) and the products (during product formation) [7]. Structural complementarity of these types are required to ensure that each working part of the machine is *coupled* to every other working part, permitting them to operate collectively as one, in a *synchronous* manner [7]. Without coupling, the required synchronicity of the multi-component assembly cannot be achieved and the machine will be unable to perform its manufacturing function. Such collective coupling also ensures that the motion of each working part of the machine is limited to a single set of optimum geometric pathways that form the only available degree of freedom. The products are manufactured when the machine cycles through this single degree of freedom. These optimum trajectories are also essential to the efficient transmission of the driving impulse through the machine, with the minimum possible energy consumed. Beyond (1)-(5) above, the following additional principles therefore also apply to kinematic manufacturing machines [8]:

(6) The required *coupling* of the machine *components* and their interaction with the starting materials and products, is typically achieved by s*tructural complementarity* involving: (i) the component parts interacting with each other, and / or (ii) the starting materials consumed and / or (iii) the product/s generated. This has the effect of:

(7) restricting the motion of the machine components to a single set of *optimum or near-optimum pathways and trajectories*, to thereby:

(8) *diminish or minimize the total energy consumed* and

(9) ensure *synchronicity* in the manufacturing process itself.

The absence of any one of the above features destroys the synchronicity of the assembly and makes the machine action impossible. A final set of attributes therefore arise from the fact that the above properties are not optional, but essential and required for the sustained functioning of the system. If even one of the above features is absent or non-optimal, the error will compound non-linearly, leading to the machine not operating properly or not operating at all. This can be likened to having one gear out of place in a clockwork mechanism, resulting in, not one less gear movement overall, but in the complete breakdown of the mechanism. For example, if the granule transport system in a compression moulding machine (Figure 2) were not correctly coupled with and synchronized to the precise time that the mould was open and empty with the ejector pin retracted, then the granules would not be correctly deposited and a moulded product could not be formed in the next cycle.

This feature of a machine is known as *synergy*, which refers to the situation where a system outcome is more than may be expected from the simple sum of its parts [8(b),9]. More specifically, it is a type of synergy that is called "*functional convergence*" in Complex System Science [8(b),9]. *Functional convergence* refers to the situation where every part of a system functions cooperatively with every other part. That is, their concerted actions and functions "*converge*" to create new capabilities that would not be possible without a high level of synchronicity. In addition to the previous points, one more crucial property of kinematic manufacturing systems is therefore:

(10) *Synergy*, deriving from system-wide cooperativity that involves all working components. This form of synergy is called *functional convergence*. We will describe and discuss synergy and functional convergence in greater detail in some of the examples referred to later in this work.

The above descriptions summarize the key principles by which industrial kinematic manufacturing machines operate. These principles are common to all such machines and, when they are simultaneously present, they unequivocally indicate the presence of a machine performing work in a repetitive and sustained fashion. That is, they indicate a kinematic manufacturing process.

In the case of industrial manufacture like that depicted in Figure 2, the inputs and outputs are physical compounds and structures. The transfer of energy is achieved by the motion of components forcing starting materials to be transformed into new products. However, the actions of biological and non-biological catalysts may also be assessed in terms of these criteria, as one would analyse the action behind a large-scale manufacturing machine.

3. Enzymes

Catalysts are species that accelerate chemical reactions without themselves being consumed in the process. Much like large-scale manufacturing machines, they transform starting materials, known as reactants or substrates, into new chemical entities, called products. The most efficient catalysts by far, are the catalysts of biology known as *enzymes*. The maintenance and creation of life on Earth depends on the ability of enzymes to facilitate chemical transformations in biochemical systems. To this end, enzymes often display truly amazing vigour, specificity, and reliability. The fact that life itself depends on the action of enzymes testifies to their remarkable power.

For example, enzymes typically generate products at frequencies from one molecule per second up to several million molecules per second, with often astonishingly high selectivity, even in the very mixed feedstock streams of biology. By comparison, man-made catalysts generally achieve nowhere near these turnover frequencies and have to rely on highly purified feedstock streams because their selectivity is so poor. That is, the active sites in man-made catalysts do not successfully target specific molecules for uptake and can be easily blocked by other molecules that are not catalysed. By contrast, most enzymes are capable of interacting with only one type of molecule within a diverse mix of compounds that typically exist in its surroundings.

Our understanding of how enzymes operate has been unfolding over more than 130 years [10]. In 1894, Emil Fischer discovered that the specificity of glycolytic enzymes indicated that they must have a particular shape into which the substrate fits [11]. He described the process of enzyme-substrate interactions as being similar to a key fitting a lock. The substrate only bound and was transformed if its shape was complementary to the docking site presented by the enzyme active site. His hypothesis came to be known as the "*Lock-and-Key*" theory. Modifications were later proposed by Haldane in 1930 and Koshland in 1958 (*"Induced-Fit"* theory) [11].

In 1946, Linus Pauling made an important advance. He noted that many enzyme active sites were likely structurally complementary to the *"optimum transition state"* of the reaction that they catalyzed [12]. He suggested that this structural complementarity probably caused the enzyme to form a transition state that was close to ideal, thereby minimizing the energy consumed in the reaction, facilitating its course [13].

One consequence of Pauling's insight was the realization that if enzyme active sites complement their optimum transition state, then they must also control the way in which substrate functional groups approach each other or disengage from each other during reaction. In fact, they must limit this approach or disengagement to trajectories and pathways that are close to the ideal since the optimum transition state represents the energetically most favourable arrangement for reaction. A diverse range of hypotheses seeking to express the concept of *optimized approach trajectories and collision pathways* have since been proposed in enzymology [14].

The concept of an "*ideal collision"* between the reactants must necessarily involve repeated, regular motion in the enzyme to mediate such collisions over and over again, with each repeat cycle generating a new product molecule. Starting in the 1970's, biochemists therefore started examining the link between repetitive conformational motion at biologically relevent temperatures in enzymes and their catalytic properties [15]. Evidence has since been collected for the existence of networks of *"coupled protein motions"* that facilitate enzymatic catalysis and that occur, in at least certain enzymes [16], on the same timescale as the rate at which product molecules are generated [15,16]. Such networks appears to comprise of fast, equilibrium thermal motions that contribute to slower conformational changes, which control the rate of production [15].

In the early 1990's, Bob Williams, a bio-inorganic chemist at Oxford University, put together the concepts of molecular recognition (via structural complementarity), optimized approach trajectories, and the role of regular, repeated conformational motion along a single degree of freedom, in his description of enzymes as "*dynamic mechanical devices*" [17].

In effect, Williams recognized that industrial kinematic manufacturing machines also display all of the above elements, albeit at a macro- and not a molecular scale. Williams further understood that the presence of these features necessarily implies that enzymes must, generally, employ a similar machine-like action. That is, enzymes must, in general, dynamically take up their substrates and guide them, during conformational flexing, through a limited set of optimum pathways, via a near-ideal transition state, to reaction [17]. They must do so in a manner analogous to the way in which kinematic manufacturing machines selectively take up starting materials and guide them synchronously along optimum pathways to form new products. These geometric motions must, moreover, be driven by the regular, repeated conformational flexing of the enzyme at ambient temperature, which is qualitatively identical to the mechanical impulse that drives industrial kinematic manufacturing machines. In analogy with Pauling's concept of enzymatic structural complementarity to the optimum transition state, product formation in industrial machines also commonly occurs within a chamber that structurally complements the product (eg. the mould of the compression moulding machine depicted in Figure 2). Swiegers later elaborated upon these proposals by showing that catalytic actions of this type must necessarily involve highly dynamic substrate-catalyst and product-catalyst binding [8,18]; this also imparts the catalyst with *functionally convergent synergies* [8(b),9].

The above general conceptualisation first proposed by Bob Williams is notable in several respects.

It is notable, firstly, for its intimation that the remarkable catalytic power of enzymes are an outcome of their machine-based manufacturing action. Like any kinematic manufacturing machine employed in industrial mass-production, the more finely tuned, geometrically

precise, and active (rapid and mobile) the molecular motions of an enzyme are, the faster, more reliable, and more sustained its mass-production.

It is, secondly, notable for the suggestion that the history of enzymology over the last 130 years may have involved the progressive discovery, in enzymes, of the various distinctive features of kinematic manufacturing machines [10]. The vigour, specificity, and reliability that characterizes enzymes may be viewed as only the most obvious, outward manifestations in this respect, as, indeed, they are for industrial kinematic manufacturng machines. That is, just as the sheer productivity of industrial kinematic manufacturing machines inspired awe at the dawn of the industrial age, so does the productive capacity of enzymes at the molecular level today.

It is, thirdly, notable for the implication that the critical role of complex, interacting, synchronous motions in enzymes had not been illuminated, at least in the early 1990's when Williams' paper was published, by readily available and standard chemical and spectroscopic techniques. Thus, for example, single crystal protein x-ray crystallography, which remains a definitive technique, provides only molecular 'snapshots' of enzymes in time, with little indication of their motion during catalysis. One may, in analogy, use the photograph of the wristwatch machinery in Figure 1 to try to understand how a wristwatch works. The development of industrial kinematic manufacturing machines was, in the same way, impeded for thousands of years by the inherent difficulty of visualising complex, interacting, synchronous motions and the remarkable synergistic effects that they may create.

4. The Catalytic Basis of Molecular Manufacturing Machines having a Kinematic Action

One may ask: what fundamental feature of catalysis is generally different in enzymes compared to abiological catalysts? In other words, what is the reason for the high catalytic performance of enzymes compared to abiological, man-made catalysts?

A key insight to answering this question can potentially be realised by comparing the processes in enzymes to those of macro-scale kinematic manufacturing machines; that is, to machines that generate a product by the successive interaction of moving parts. In such a manufacturing machine, as noted previously, the great production capacity is achieved by limiting and synchronising the motion of components to a single, optimum degree of freedom which comprises the manufacturing action. Likewise, enzymes may possibly control and direct the movement of substrates, causing them to collide with, or disengage from each other at the optimum point of transition state formation. That is, the transition state may arise not as a random statistical probability due to thermal motion but because the enzyme moves under the impetus of thermal motion in such a way as to create ideal collisions between reactants. Like industrial kinematic manufacturing machines, enzymes may possibly control and constrain how substrates approach and interact with each other at the optimum point of transition state formation. That is, they may generally create "ideal" or near ideal collisions between reactants, with their overall rate of catalytic turnover determined by their rate of conformational flexing along the single degree of freedom. By contrast, man-made catalysts would not generally have a capacity for such control; they typically have multiple degrees of freedom available to them and are unconstrained in this respect.

According to collision theory, reactants form products by colliding with each other. The overall rate of reaction (k) is given by the Arrhenius equation (equation (1)), which consists

of two factors: (i) the frequency with which the reactant molecules collide with each other (the pre-exponential term A, known as the *"Collision Frequency"*), and (ii) the proportion of those collisions that are sufficiently energetic to result in product formation (the exponential term, $-E_A/RT$, where E_A is the *"Activation Energy"* of the reaction) [8(a),18].

$$k = A \exp(-E_A/RT) \qquad \ldots(1)$$

The rate of all chemical reactions, including catalyzed reactions, are controlled by whichever of the above factors is rate limiting, the collision frequency (A) or the exponential term ($-E_A/RT$) containing the activation energy (E_A).

In the case of a kinematic manufacturing machine operating at the molecular level, the reaction rate would clearly have to be determined by the collision frequency (A), since this is what the catalyst would do – it would create near-ideal collisions over and over again, with each collision generating a product molecule. By contrast, a man-made catalyst that is not constrained to motion along a single degree of freedom, would not be limited by the collision frequency but rather by the proportion of collisions that are successful – that is, by the exponential term, $-E_A/RT$, and the activation energy (E_A) of the reaction.

In the case of enzymes, this hypothesis may potentially be enhanced by observations made by Michaelis and Menten in the early 20th Century. They discovered that the kinetics of enzymes generally depends on a pre-reaction enzyme-substrate complex, termed the "Michaelis Complex". If enzymes indeed act as kinematic molecular manufacturing machines, then the Michaelis complex is simply the molecular machine after it has taken up a reactant substrate and while it is going through the process of conformationally flexing along

its single degree of freedom leading to product generation. The formation of the Michaelis complex and the switching between it and the free-standing enzyme state would thereby be rate limiting. By comparison, the kinetics of abiological catalysts are not generally limited by a pre-reaction catalyst-reactant species, and are instead governed by their activation energy, E_A, in the exponential term of the Arrhenius equation [8,18].

5. Abiological Catalysts that Employ a Kinematic Manufacturing Action

The question that now arises is whether any man-made catalysts exhibit a kinematic manufacturing action at the molecular level? If such species exist, they potentially confirm that molecular-level kinematic manufacturing processes are possible and provide further insights into them. Such species would, however, likely have been created or discovered by accident and not by design. As such, they would be rare.

Following an exhaustive review of the catalytic literature over a number of years, several man-made catalysts that appear to display the key characteristics of a kinematic mode of action, have been identified. Because the mechanism of action of many of the catalysts has not been fully clarified, it is often not possible to say with certainty whether a particular catalyst employs a kinematic action or not. In such cases, one can only look at the distinctive features that the catalyst exhibits or, alternatively, at the outcomes that it achieves, and determine if these are consistent with such an action.

The present section (Section 5) reviews two catalyst systems whose mechanisms have been subjected to very detailed investigation and that clearly do employ a molecular kinematic manufacturing action. The following section (Section 6) reviews several illustrative

examples of catalysts that display the distinctive features of a kinematic manufacturing action, but whose mechanisms have not been illuminated in full detail. Such catalysts are strongly inferred to employ a kinematic manufacturing action. The section thereafter (Section 7) reviews catalysts whose product outcomes are indicative of, or consistent in some way with molecular catalysis involving a kinematic mode of action. Such catalysts may well employ a kinematic manufacturing action

A note on forthcoming Figures 3 and 5-10: As will be appreciated, it is not a simple matter to depict dynamic chemical processes that operate in parallel and that interact with each other at very specific points in time. To best illustrate the processes at play in the examples below, we have therefore provided Figures 3 and 5-10 that set out to illustrate each system using the same elements that were employed in preceding Figure 2 (which showed the operation of a typical compression moulding machine). That is, each of Figures 3 and 5-10 have been specifically formulated to allow for ready comparison with Figure 2; they comprise of:

(i) a "*Process Flow Diagram*" that depicts the sequence of steps that the starting material is taken through during the manufacturing process. The Process Flow Diagram comprises the 'blocks' across the very top of each figure, commencing with the starting materials (on the left) and ending with the final product (on the right).

(ii) Below the Process Flow Diagram, in the middle of each figure, is shown the key cyclical process involved in the manufacturing action.

(iii) At the bottom of each figure, the steps involved in the key cyclical process have been depicted using a simple schematic. We have further introduced dashed arrows between the Process Flow Diagram at the top of the figure and the schematic at the bottom of the figure, to show the correlation between these two representations of the manufacturing action.

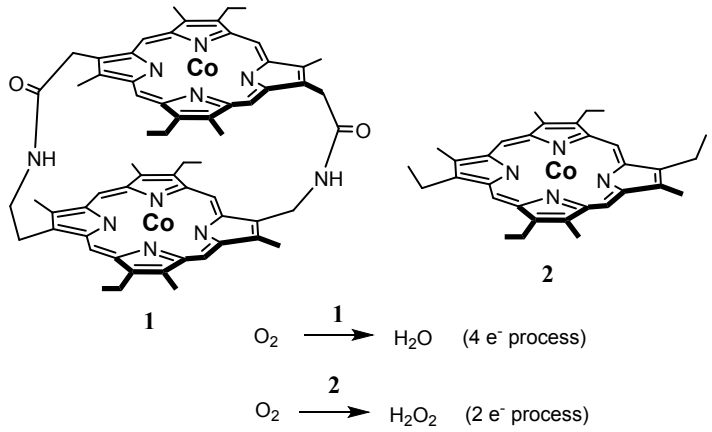

Scheme 1. *Di-cobalt porphyrin oxygen reduction catalysts.*

5.1 Cofacial Diporphyrin Catalysts

Starting in 1977, a series of catalysts were developed that involved two metalloporphyrins in an eclipsed face-to-face arrangement that was constrained to flex longitudinally. Several of these catalysts employed a catalytic action in which the facing metalloporphyrins acted cooperatively (convergently) to reduce dioxygen, O_2, to two water molecules, H_2O.

For example, dicobalt porphyrin **1** (Scheme 1) catalyzed the 4-electron reduction of O_2 to H_2O at pH <3.5 and at potentials negative of 0.71 V (vs. NHE), when adsorbed on a graphite electrode [19,20]. By contrast, the corresponding monomer **2** catalytically generated the 2-electron product, H_2O_2 under similar conditions. Studies showed that **1** did not catalytically convert H_2O_2 into H_2O and therefore did not simply perform successive reductions. Moreover, **3** (Scheme 2), which differs from **1** only in having greater conformational freedom due to the presence of an extra carbon atom in its linkers, generated, exclusively, H_2O_2 in a 2-electron process [20,21]. It was concluded that the nature of the linker in **1**, which limited conformational flexing to oscillation about an eclipsed face-to-face arrangement, were crucial

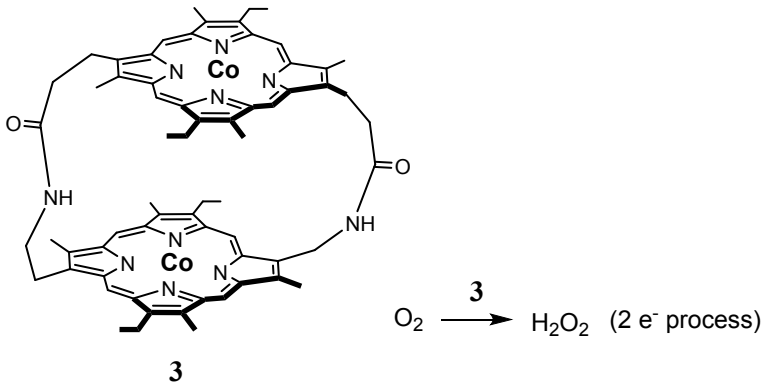

3

Scheme 2. *Di-cobalt porphyrin oxygen reduction catalyst that is free to flex about more than a single degree of freedom.*

to the catalysis. That is, constraining the conformational flexing of the molecule to a single- or near-single degree of freedom appeared to have created the key catalytic effect.

Further studies in this respect involved the incorporation of a rigid aryl linker between the cofacial porphyrins, as depicted in **4** and **5** (Scheme 3) [22,23]. The linker constrained the Co porphyrins even more severely to a single mode of rapid, repeated longitudinal flexing, termed "Pac-man" flexing (Scheme 4) [23], about an eclipsed face-to-face conformer. As was the case for **1**, catalysis by **4** and **5** facilitated exclusively the 4-electron

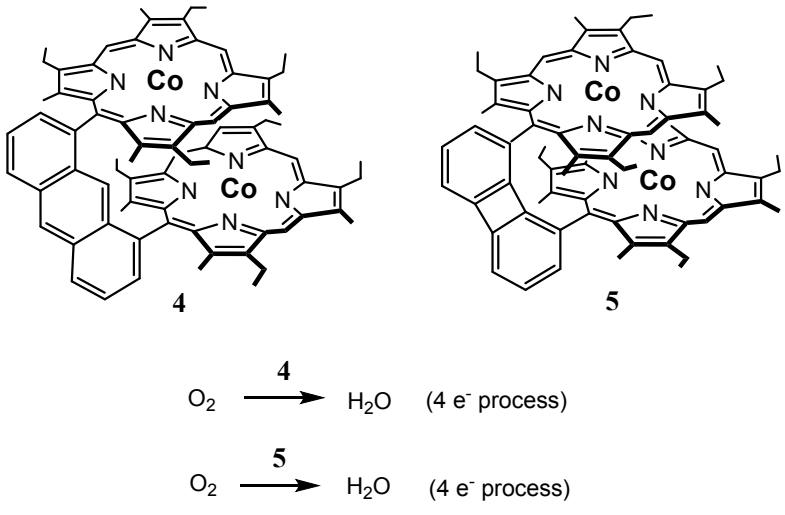

Scheme 3. *Di-Co porphyrin O_2 reduction catalysts that are constrained to flex about a single degree of freedom.*

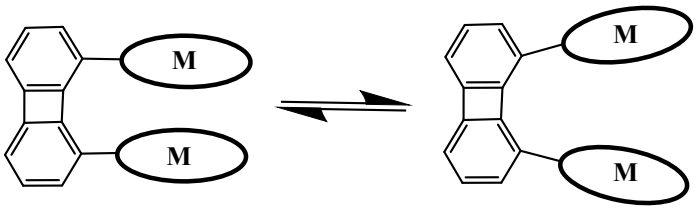

Scheme 4. *"Pac-man"-type regular, repeated flexing in* ***4*** *and* ***5****.*

process for oxygen reduction. Clearly, maximum selectivity for the 4-electron reduction was achieved by constraining conformational motion to a single degree of freedom involving regular, repeated opening and closing of the "bite" of the cofacial metalloporphyrins.

A more complete explanation was afforded by the later discovery that only one redox metal was, in fact, needed to achieve selectivity for H_2O [24]. Both the monocobalt diporphyrin **6** (Scheme 5), which is the partially demetallized version of **1**, and a cobalt-aluminium diporphyrin, also catalyzed 4-electron reduction, although only in parallel with the competing 2-electron process [25]. The second Co ion in **1** was thereby revealed to act largely as a Lewis acid during the catalysis [22(a),24].

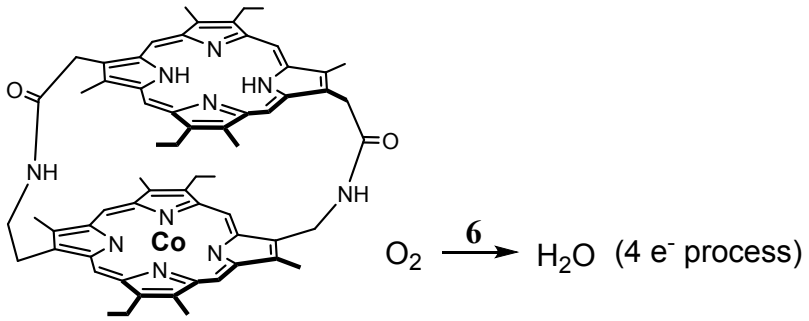

6

Scheme 5. *Mono-cobalt porphyrin oxygen reduction catalyst.*

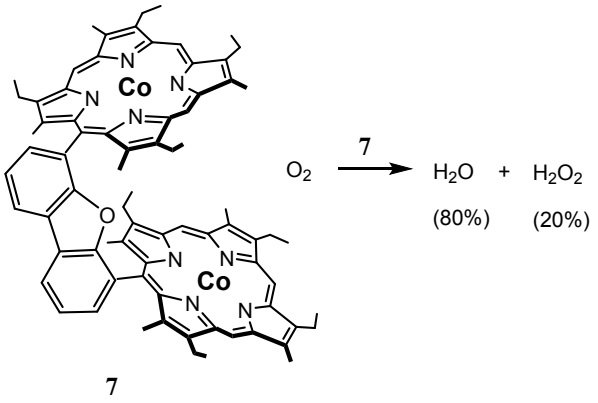

7

Scheme 6. *Dicobalt porphyrin oxygen reduction catalyst with benzofuran linker.*

Studies also showed that other cofacial cobalt diporphyrins catalyzed the formation of water from oxygen, although also only as a co-product with H_2O_2. For example, a diporphyrin containing a dibenzofuran linker **7**, which led the two rings to be angled at 56.5° with respect to each other on average, catalyzed the conversion of 80% of the O_2 reactants to water [23]. This was despite an average Co-Co distance of 8.624 Å, which is substantially longer than the average 3.73 Å in **4**. The study's authors ascribed the catalytic effect to longitudinal flexing, which allowed the molecule to "bite" down on the O_2 substrate. Like **1**, **4**, and **5**, conformational oscillation about the eclipsed conformation was undoubtedly still highly populated in **7**.

Mechanistic studies showed that when O_2 binds to the cofacial dicobalt porphyrins, it does so in the pocket formed between the metals, where it is initially bound as a μ-superoxide species that bridges the two Co ions [26]. The actual catalyst proved to be the $Co^{II}Co^{III}$ form of **1**, with the second metal (the Co^{III}) acting as a Lewis acid [22(a)].

The extreme sensitivity of the catalytic reaction to the nature of the conformational flexing in this system, indicated that the O_2 reactant binds only very transiently to both of the Co ions

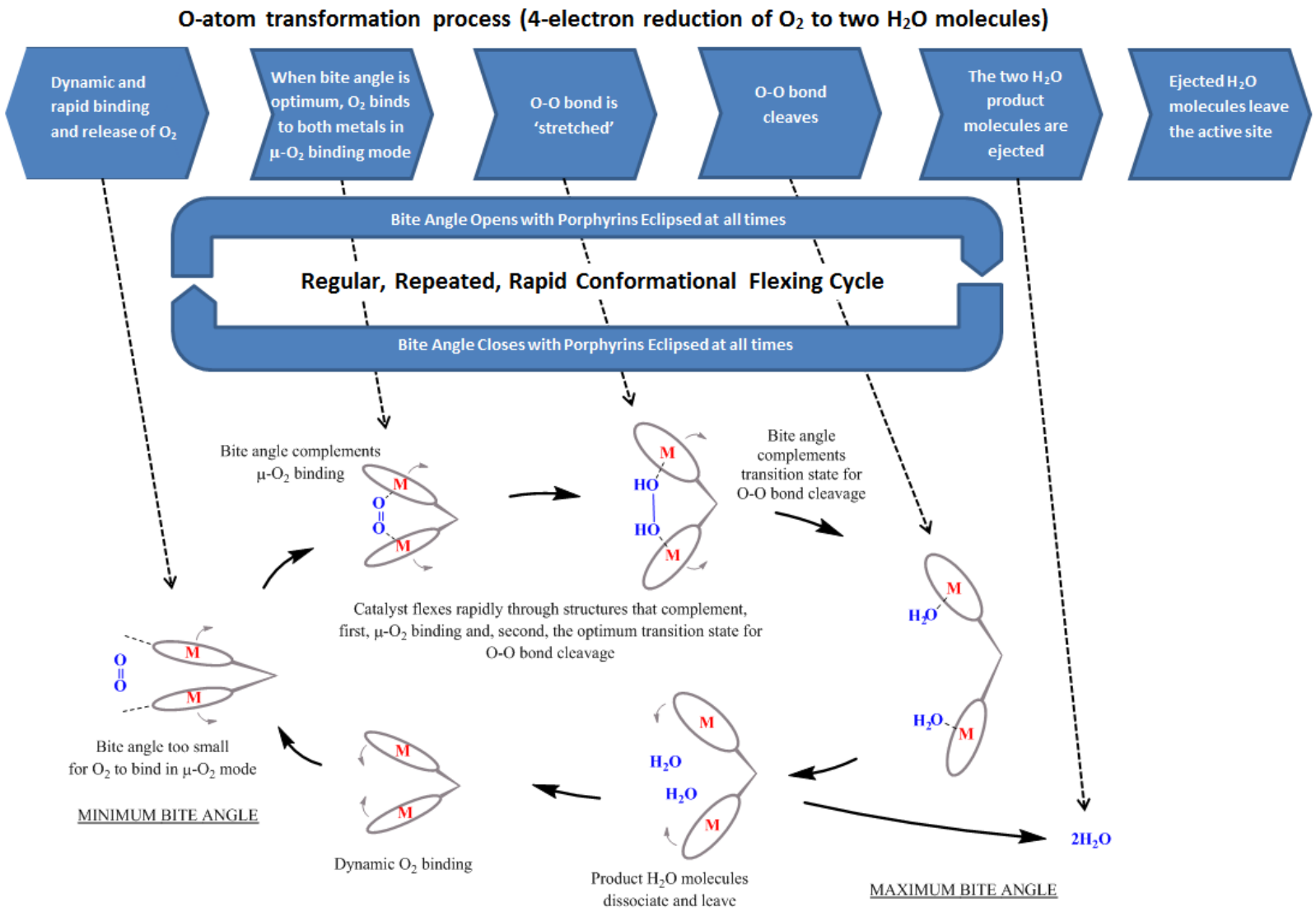

Figure 3. *Schematic of the repetitive kinematic cycle for 4-electron reduction of O_2 into H_2O by eclipsed cofacial diporphyrins (M=Co) during 'pac-man'-type rapid conformational oscillation. Note that the independent processes of: (i) transient μ-O_2 binding and (ii) opening of the bite angle by the eclipsed porphyrins, must be synchronized in order for the catalyst to operate successfully. If the diporphyrins are not eclipsed when the bite angle opens towards its maximum, then μ-O_2 binding leading to O-O bond cleavage is not possible and H_2O_2 is instead released in a 2-electron reduction process without O-O cleavage.*

simultaneously. If, during that brief period of time of μ-O_2 binding, the catalyst opened its bite by flexing along a longitudinal, eclipsed pathway, then the O_2 would be, quite literally, pulled apart. That is, the O-O bond was cleaved by the process of progressively increasing the separation between the two O-atoms during the opening of the bite, whilst maintaining an eclipsed arrangement. By contrast, if the catalyst was unable to pull the O_2 apart in the brief period that it was bound to both Co ions (due, for example, to a non-eclipsed conformational arrangement), then a slower, 2-electron process occurred instead, yielding H_2O_2 as the reaction product, in which the O-O bond remained intact.

Figure 3 schematically illustrates these processes in catalytic 4-electron reduction by a cofacial diporphyrin like **1**, **4**, or **5**. The top-most set of blocks depict the processes that the O-atoms undergo (from O_2 reactant to H_2O product). Below that in the middle of Figure 3, is shown the cycle of conformational flexing of the cofacial diporphyrin that occurs in parallel. The schematic at the bottom of Figure 3 shows the key individual catalytic steps during the flexing cycle of the cofacial diporphyrin.

As shown in Figure 3, during this flexing cycle, the "bite" of the cofacial diporphyrin opens and closes repetitively. During this process, O_2 dynamically binds and releases the Co ions. However, it is only at one particular instant in time during the bite opening process that the bite is optimum for O_2 to bind simultaneously with both Co ions in a μ-O_2 binding mode. That is, at this one juncture in time during the bite opening process, the cofacial diporphyrin structurally complements (and thereby facilitates) binding of the O_2 reactant at both metal ions simultaneously.

Immediately after μ-O_2 binding, the bite of the cofacial diporphyrin opens further, stretching and ultimately rupturing the O-O bond (provided the metal ions remain eclipsed). That is, the flexing cycle thereafter rapidly passes through a structure that complements the optimum transition state for O-O bond cleavage, facilitating that reaction. During this process, it is critical that the O_2 remains bound to both metals. This can only occur if the metal ions remain eclipsed while the bite angle opens through this structure.

These catalysts therefore operate by flexing rapidly through, first, a structure that complements μ-O_2 binding by the reactant O_2, and then, secondly, a structure that complements the optimum transition state for O-O bond cleavage.

In effect, when the metal ions remain eclipsed, the catalyst ensures that the two independent, dynamic processes of conformational flexing of the diporphyrin framework (during 'bite opening') and μ-O_2 binding, are synchronized with each other [18]. In other words, the 4-electron reduction reaction only occurs if the regular, repeated process of bite opening by the catalyst overlaps in time with the process of μ-O_2 binding by the catalyst [18]. This is achieved by maintaining the diporphyrins in an eclipsed arrangement during bite opening, as they do in **1**, **4**, and **5**.

When an eclipsed structure is not strictly preserved, as in **2** or **3**, then μ-O_2 binding cannot be maintained during the critical period that the bite opens towards its maximum angle. The diporphyrin therefore does not pass through a structure that complements the optimum transition state for O-O cleavage with a bound μ-O_2 reactant in place. Instead the O_2 disassociates as the 2-electron H_2O_2 product, in which the O-O bond remains intact. The

‘collision frequency’, which is defined in this case as the rate at which the O atoms in O_2 are pulled apart, thereby falls to zero.

The processes depicted in Figure 3 are analogous to those of a large-scale industrial kinematic manufacturing machine, as illustrated in Figure 2.

Firstly, the process is dependent upon a regular, repeated, and rapid cycle of conformational flexing that occurs spontaneously at the temperature employed during the catalysis. This motion is constrained to occur along a single degree of freedom.

Secondly, during flexing, the catalyst selectively takes-up and transports the O_2 reactant in a state suitable to facilitate O-O bond cleavage in a next step. This is qualitatively similar to the granule transport process in a compression moulding machine of the type in Figure 2, taking up a particular quantity of granules and pre-heating them while transporting them to the mould.

Shortly thereafter, the suitably-bound O_2 reactant is, thirdly, passed through a structural framework that complements the optimum transition state for O-O cleavage, causing it to undergo 4-electron reduction, generating two H_2O molecules. This is qualitatively similar to a compression moulding machine passing granules of a thermoset resin through a mold that complements the structure of the desired final product, as depicted in Figure 2.

During subsequent flexing, the H_2O molecules dissociate from the Co centers and are ejected, allowing the cofacial diporphyrin to close their bite back to the starting point for the next cycle. This is similar to the ejection process in a compression moulding machine.

The constrained nature of the conformational flexing cycle is, moreover, needed in order to favour synchronocity in μ-O_2 binding at the precise instant that the bite passes through a structure that complements the transition state for O-O rupture. In this way, the two cofacial porphyrins are able to act in a cooperative, "convergent" manner.

The synergy achieved in eclipsed cofacial diporphyrins like **1**, **4**, and **5** that facilitate 4-electron reduction to H_2O, is evidenced by a new capability, namely, the ability to cleave the O-O bond in O_2. That capability is not available, even in a minor capacity, to either the individual components of the diporphyrin (eg. **2**) or to assembled components that flex inopportunely (eg **3**). In other words, the new capability arises solely because of the dynamic motion of the catalyst components along a single, well-defined, near-ideal, degree of freedom, and its synchronization with μ-O_2 reactant binding.

This process can also be understood in the sense that there is one set of optimum component trajectories that work only when they are synchronized in their interaction with the other components. In the same way, if one were to, for example, alter the length of the stroke of the pistons in an internal combustion engine, then the input of gasoline and the spark for combustion, would not be synchronized with the motion of the cylinder. The desired work would then be done in suboptimal coexistence with other processes, leading to partial combustion or even complete breakdown of the engine.

Precisely the same principles therefore apply in macro-scale industrial kinematic machines, which is why they must be so carefully machined and why they have to be designed to utilize

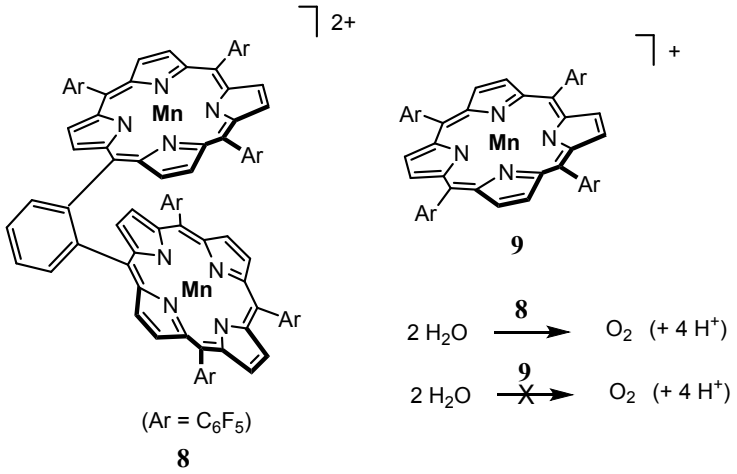

Scheme 7. *Di-manganese porphyrin water oxidation catalysts.*

structural complementarity. As in **1**, **4**, and **5**, the effectiveness of their overall kinematic process relies on carefully synchronized spatial and temporal features.

In comparison to cofacial diporphyrin catalysts for oxygen reduction there are fewer studies on similar systems for the reverse reaction, namely, water oxidation. One notable exception however, is the cofacial dimanganese diporphyrin catalyst **8** (Scheme 7), which catalyzed the oxidation of H_2O into O_2 [27(a)].

A similar machine-like effect to that noted above appears to exist in **8**. For example, while **8** was a water oxidation catalyst, its comparable monomer, **9**, was not. The mechanism of water oxidation by **8** was, moreover, proposed to involve hydroxide binding at the Mn^{III} centers, followed by the formation of a Mn^{IV}-O-O-Mn^{IV} intermediate during closing of the diporphyrin bite, which led, in turn, to O_2 formation and release.

A mechanism involving O-O bond formation during conformational flexing was supported by studies showing that the spatial organization and proximity of the Mn^{III} centers to each other were critical to the catalytic effect [27(b)].

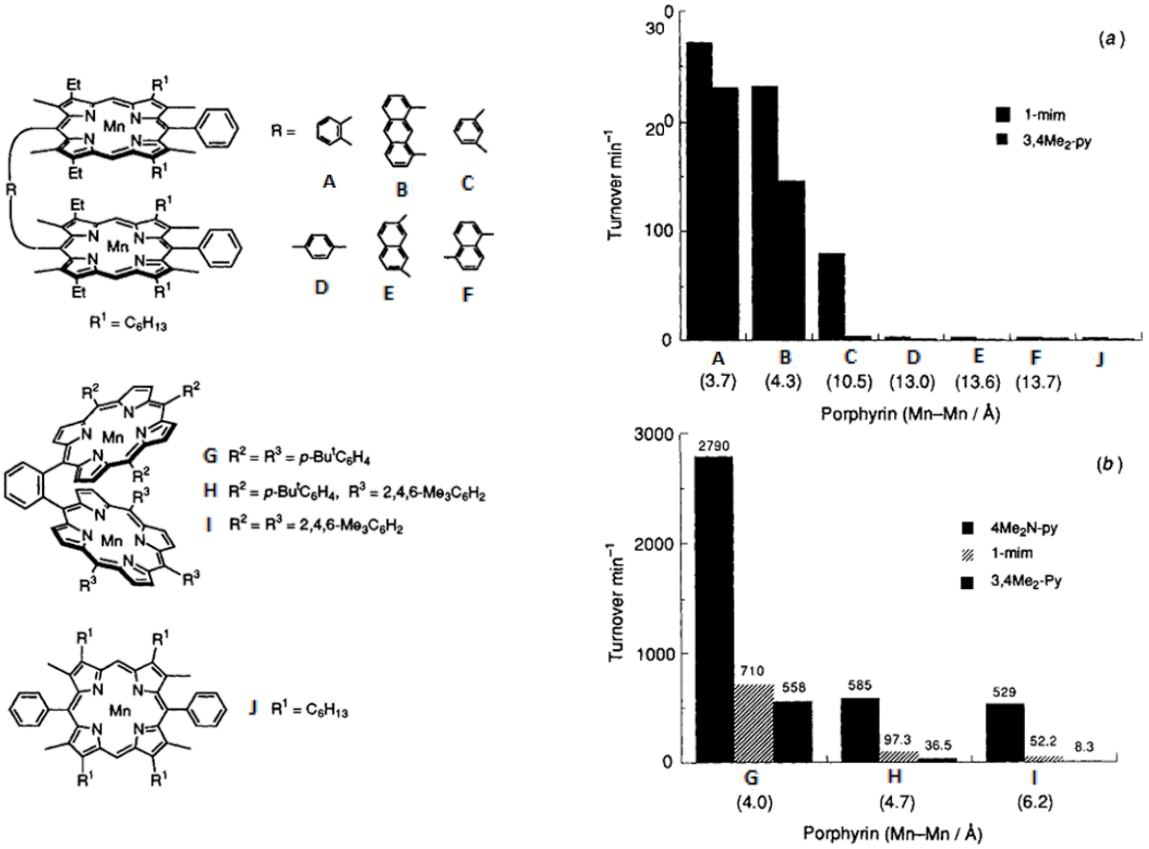

Figure 4. *Turnover frequencies with respect to Mn-Mn distance for: (a) co-facial Mn di-porphyrins having various aromatic and fused aromatic linkers, and (b) variants of* ***8*** *with different porphyrin functionalizations. (Reproduced with permission from reference [27(c)]).*

To better understand the processes at work, Naruta and colleagues compared catalytic rates in variants of **8** having either different linkers between the porphyrins or meso / β-pyrrolic functionalization on the porphyrins (Figure 4) [27(c)]. Special attention was paid to the average Mn-Mn distance in these cases. As can be seen in Figure 4, the systems examined tended to either display strong catalytic activity (left of Figures 4(a) and (b)), or no catalytic activity at all. This would be consistent with a kinematic mode of action. The findings also confirmed the critical nature of the average Mn-Mn separation with only one catalyst performing at turnover rates of several thousand molecules per minute compared to several hundred at best by the other variants under the same conditions. When the Mn ions were too distant or not in an eclipsed arrangement, no catalytic reaction occurred.

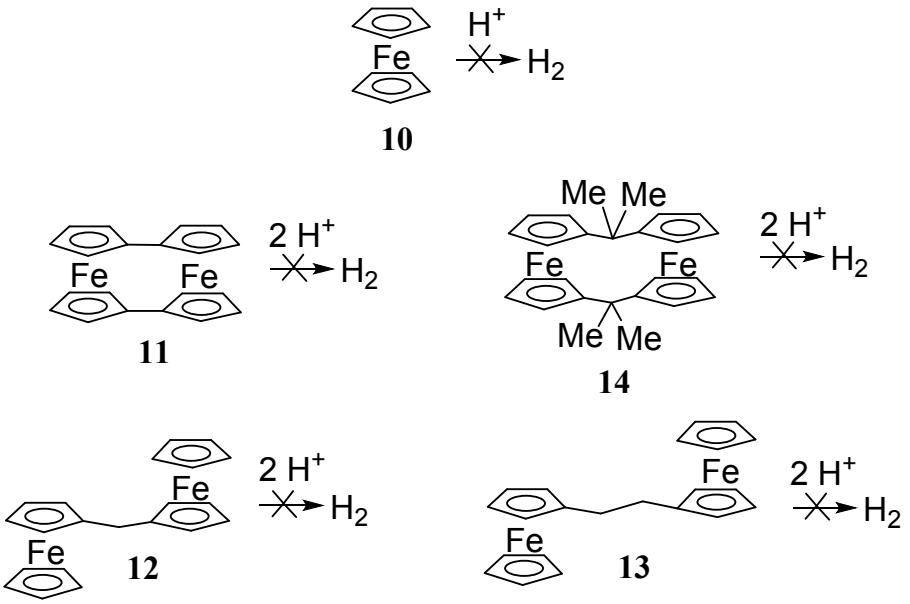

Scheme 8. *Ferrocene species that are not hydrogen generation catalysts*

Several other multi-centered catalysts involve metalloporphyrins. For example, several copper-imidazole capped metalloporphyrins have been reported to be catalysts of the 4-electron reduction of oxygen to water at physiological pH [28-33]. Cofacial diporphyrins have also been widely used as proton reduction and hydrogen oxidation catalysts, as well as in studies examining the catalytic interconversion of dinitrogen and its nitrogen hydrides [22(a),34,35].

5.2 Tethered Ferrocene Catalysts

A wide range of mono- and di-ferrocene compounds have been prepared and studied, including **10**-**14** (Scheme 8) [36,37]. None of these species has ever been reported to display any sort of catalytic properties whatsoever. However, in 1973, Bitterwolf and Ling discovered that the di-ferrocene **15a** (Scheme 9), which undergoes very rapid conformational flexing at room temperature, catalytically converted strong non-oxidizing acids to dihydrogen, H_2, in the presence of a sacrificial $SnCl_2$ reductant. The $SnCl_2$ was needed to quantitatively recycle

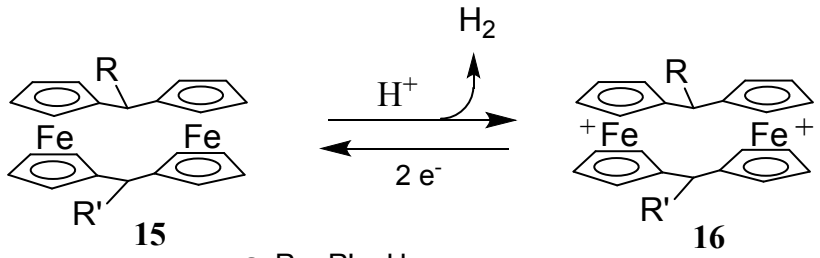

a: R = R' = H;
b: R = Me, R' = H;
c: R = Me, R' = Me-p(styrene)

Scheme 9. *Di-ferrocenes that are hydrogen generation catalysts*

the dication **16a** back to **15a** to thereby close the catalytic cycle [36]. Further studies showed that the related ferrocenes and di-ferrocenes **10**-**13** did not catalyze the same transformation [38]. However, the mono-methyl-substituted di-ferrocene **15b** (Scheme 9) also catalyzed hydrogen production, albeit at a slower rate, in accord with its slower rate of conformational flexing at room temperature [38].

Interestingly, the equivalent di-methyl-substituted analogue **14** (Scheme 8), which differed from **15b** only in the presence of two methyl groups rather than one on the bridgehead carbons, was catalytically entirely inactive [38]. This molecule exhibited an extremely slow rate of conformational flexing at room temperature due to the presence of the bulky methyl substituents.

The most stunning results arose when **15** was tethered to a methylpolystyrene coating deposited on a *p*-type silicon substrate, which was tested in 1 M strong acids [39]. Under illumination with sunlight, the resulting photoelectrode **15c**/Si displayed an onset potential 250 mV anodic of the most positive potential for hydrogen generation on the industry-best catalyst, platinum, and generated 5 molecules of H_2 per second continuously for over 5 days of testing without any decrease in activity. In uncoated form, the silicon was totally inactive. That equated to more than 2.16 million H_2 molecules produced per molecular catalyst **15c** without any de-activation. In a separate experiment, individual molecules of **15a** in acid

solution readily turned over >1,000,000 H_2 molecules without any notable loss of activity [38,40].

The di-ferrocenes **15** are therefore, surprisingly, not only catalysts of hydrogen generation, but extraordinarily active and long-lived ones too. Their sheer durability and activity indicates an excellent catalytic selectivity that prevents the formation of nonfunctional intermediates and avoids deactivation.

As a result of these remarkable feats, there was significant interest in the mechanism by which **15a-c** catalyzed hydrogen formation and why this mechanism did not operate in **10-14**.

NMR and cyclic voltammetry studies showed that, in acid solution, protons (H^+) transiently bound the Fe atoms in **15a**, with the two ferrocenes separately protonated at each Fe center [44-46]. The binding at each Fe center involved a dynamic equilibrium, which included direct Fe-H binding, as well as protonation at the ring carbons, as depicted in Scheme 10 [41,42]. The exchange processes were too rapid to be resolved on the NMR timescale, even at -122 ^oC [41,43].

Theoretical studies showed however that, when bound to the ferrocene Fe atoms, most of the positive charge of the H^+ ions relocated to the metal, causing them to be, effectively,

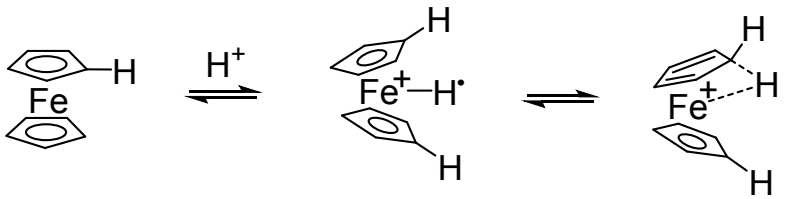

Scheme 10. *Protonation of ferrocene is highly dynamic*

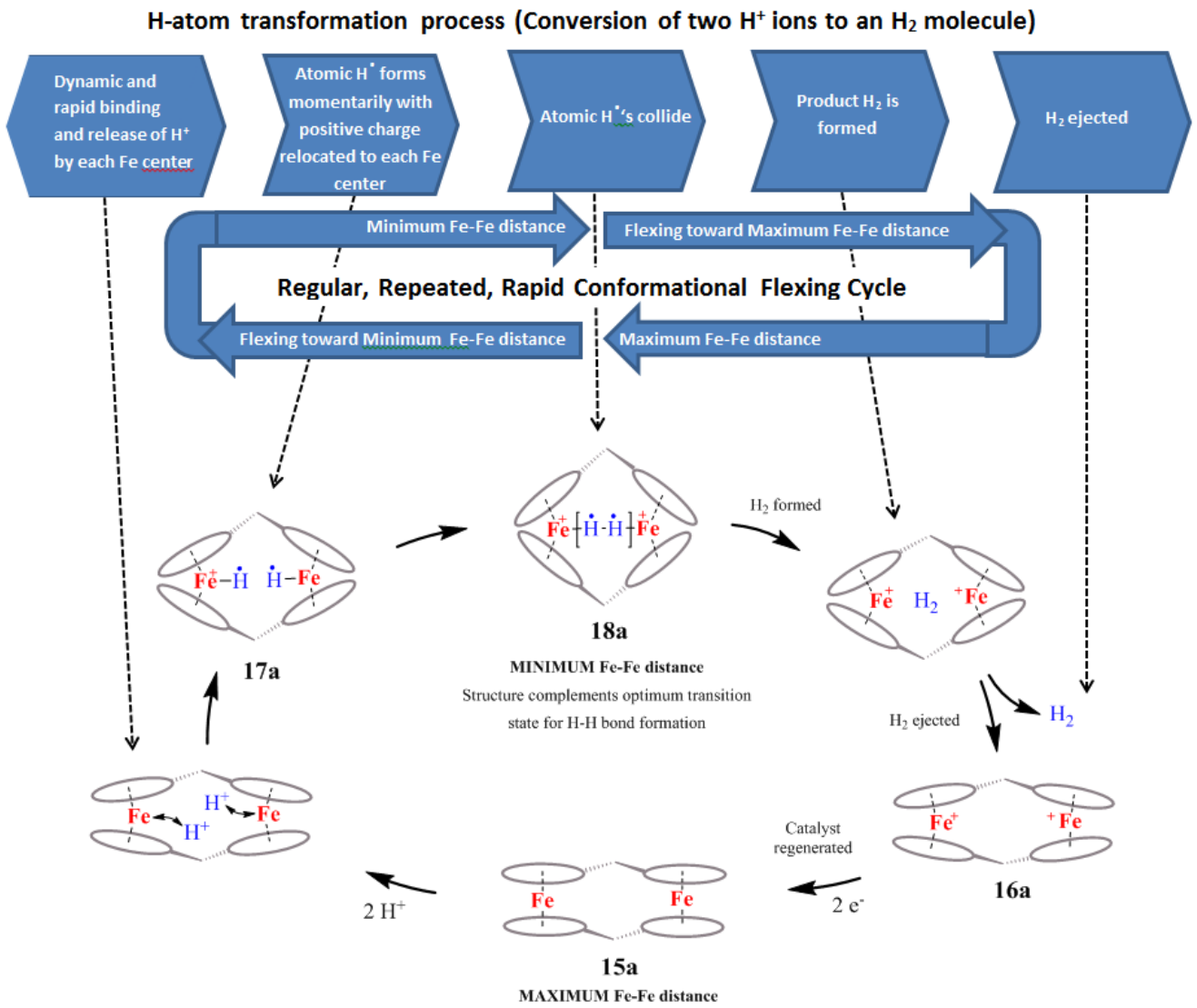

Figure 5. *Schematic of the repetitive kinematic cycle for conversion of H^+ to H_2 during rapid conformational flexing by [1.1]ferrocenophane* ***15a****. Note that the independent processes of: (i) transient H^+ binding at each Fe center and (ii) the conformational flexing of the biferrocene, must be synchronized in order for the catalyst to operate. This only occurs if the biferrocene flexes rapidly about a structure that complements the optimum transition state of the reaction. Other mono- and bi-ferrocenes that do not flex about this structure, like* ***10-13****, or that flex too slowly, like* ***14****, are inactive. The biferrocene* ***15b****, which flexes slower than* ***15a*** *but faster than* ***14****, displays lower activity.*

activated atomic hydrogen (H•) [41,43]. An X-ray crystal structure, along with molecular modelling, showed the Fe···Fe distance in **15a** to oscillate between 3.4 – 4.8 Å during flexing [46]. H_2 formation by **15a** therefore effectively involved the homolytic combination of two Fe-bound atomic hydrogen atoms during flexing (as illustrated in **18a** (Figure 5)) [36,47,48].

The extraordinary catalytic capability of **15a** and **15c** consequently arose from synchronicity in the two, independent, dynamic processes of proton binding and conformational flexing [18]. Figure 5 illustrates the pertinent processes at play in this class of catalyst. The blocks at the top of Figure 5 depict the steps by which hydrogen atoms are transformed, from H^+ ions to H_2 molecules. The cycle below that in Figure 5 and the schematic at the bottom of Figure 5 illustrate the process of regular, repeated conformational flexing by **15a**, from the maximum Fe-Fe distance at the bottom of the Figure to the minimum Fe-Fe distance above it.

As can be seen, there are two independent processes that must be synchronized for biferrocenes to catalyze hydrogen reduction, namely: (i) transient and dynamic H^+ binding at each Fe center and (ii) conformational flexing. In the case of **15a**, there was clearly a high likelihood that both ferrocenes would be protonated (and bearing, effectively, atomic hydrogen) at the point in the flexing cycle at which they would be favored to collide with each other (depicted in **18a**).

This was because the biferrocene structure flexed very rapidly along a single degree of freedom, which incorporated a structure that complemented the optimum transition state for H-H bond formation (depicted in **18a**). Thus, while each ferrocene engaged in a dynamic protonation that resulted in the momentary formation of a highly reactive atomic hydrogen species (**17a**), the speed and the nature of the flexing was such that these species were immediately thereafter brought into reactive contact with each other (**18a**) as the biferrocene flexed through a structure that complemented the optimum transition state for H-H bond formation. In effect, the rapidity and the trajectory of the regular, repeated motion

of the ferrocenes was such as to sequester the short-lived atomic hydrogen species formed on the Fe centers within a H_2 molecule.

Kinetic studies [47,48] of **15a** produced data that was later [18] found to conform to a Lineweaver-Burke plot with K_M ca. 0.2 μM. Lineweaver-Burke plots are indicative of Michaelis-Menten kinetics, which, as noted earlier, may possibly be characteristic of a kinematic molecular manufacturing action.

By contrast, in the comparable species **10**-**13**, the likelihood that the above independent processes will be synchronized falls to zero, meaning that they are catalytically totally inactive. This is because of the absence in these species of regular, repeated and rapid conformational flexing about a single, optimum degree of freedom, which incorporates a structure that complements the optimum transition state for H-H bond formation. In effect, **10**-**13** provide no mechanism by which to capture the transient and short-lived atomic hydrogen species formed on the Fe centers.

The importance of the rapidity of flexing by **15a** was demonstrated by the effect on the catalysis, of substituting methyl groups on its bridgehead carbons. When one methyl group was substituted on each

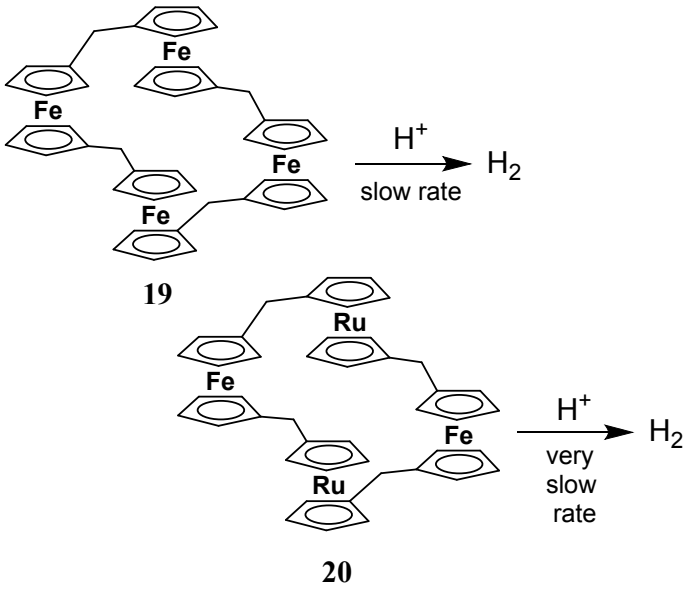

Scheme 11. *Tetra-metallocenes that are hydrogen generation catalysts*

bridgehead carbon, the resulting biferrocene **15b** flexed more slowly at room temperature, thereby yielding a substantially slower rate of catalysis [38]. The presence of two methyl groups on each bridgehead carbon in **14**, slowed the flexing sufficiently to completely halt the catalytic effect [38].

The rate of flexing of the tetra-metallocenes **19** and **20** (Scheme 11) also influenced their catalysis [42,44]. In **19**, four ferrocenes are tethered in an arrangement that allows opposing Fe centers to alternately mediate collisions between attached hydrogen reactants during flexing at room temperature. Because of the size of this molecule, its rate of flexing is slower than **15a**. This resulted in a very much slower rate of catalytic hydrogen generation from 1 M strong acids. The mixed tetramer **20** involving opposing ferrocene and ruthenocene groups, displayed an even slower, but still measurable catalytic rate [44]. The catalysis was entirely due to interactions between opposing protonated ferrocenes during flexing. Ruthenocene is substantially more basic than ferrocene and therefore more readily protonated. However, it favors 2-electron and not 1-electron oxidation and is consequently unable to form the catalytically required +1 oxidation state intermediate [45]. In acidic solution, the ruthenocene units became protonated, but did not eliminate H_2.

In **15a-c**, we therefore have further examples where, in accord with the principles of kinematic manufacturing, a powerful catalytic effect was created by dynamic and selective reactant binding synchronized with rapid, repeated and regular conformational flexing along a single, optimum degree of freedom. As in the previous section, the catalyst acted to, first, selectively bind and activate the reactant while it then, secondly, rapidly transported it along the shortest available trajectory through a structure that complemented the optimum transition state for the reaction. Further flexing after H_2 formation, back to the starting point, caused the H_2 to be dissociated from the Fe centers and ejected from the active site, opening the way to the next cycle. The resulting synergy created a new capability; catalytically unremarkable ferrocene groups were transformed into potent and long-lived hydrogen-generating catalysts. Without the above features, as in **10**-**14**, catalytic transformation was impossible.

6. Abiological Catalysts that Display Key Features Expected in Kinematic Molecular Manufacturing Machines

As noted above, the mechanisms by which many catalysts operate have not been fully clarified, making it difficult to establish whether they employ a kinematic manufacturing action or not. The presence of some of the more distinctive features described in Section 2 above, nevertheless, strongly support the presence of such an action in certain such catalysts. This section reviews catalysts that display features which are highly characteristic of a kinematic manufacturing action.

6.1 Supramolecular Catalysts

A vast literature exists of supramolecular catalysts, including bifunctional supramolecular catalysts. The most common receptor sites used in such catalysts are inclusion-promoting or supramolecular species, like macrocycles, crown ethers, cyclodextrins, and the like. The binding interactions employed are typically dynamic in character, such as hydrophobic-hydrophilic interactions. Reviews of such catalysts are available [50-53].

Many supramolecular catalysts display at least some of the features of kinematic manufacturing machines, including: (1) dynamic catalyst–reactant binding interactions, (2) high catalytic selectivity and activity, (3) apparent structural complementarity with the optimum transition state of the reaction, (4) a high level of cooperativity in the catalyst components in order to achieve the catalytic action, (5) a transformation of unremarkable chemical groups into often notably powerful catalysts, (6) minor changes in the structure / connectivity / flexing of the catalyst completely destroy the catalytic effect, and (7) Michaelis–Menten kinetics. However, the mechanisms employed by such catalysts have typically not been investigated in detail. They are therefore not understood well enough to be able to

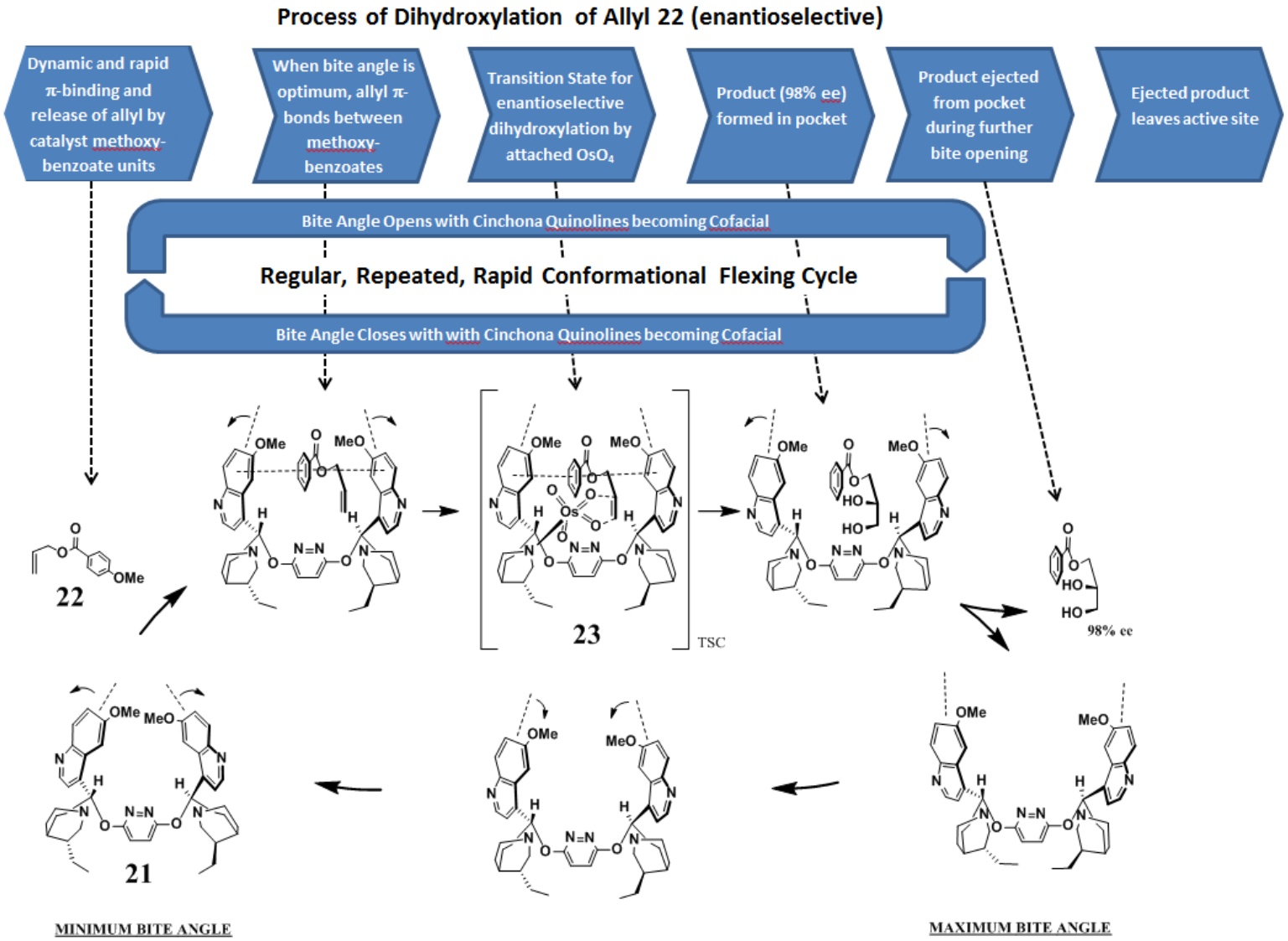

Figure 6. *Likely repetitive kinematic cycle for enantioselective asymmetric dihydroxylation of* ***22*** *during rapid conformational flexing by bis(cinchona) alkaloid catalyst* ***21****. Note that the independent processes of: (i) directionally-specific allyl π-binding, (ii) bite opening and closing of* ***21****, and (iii)* OsO_4 *incorporation, must be synchronized in order for the catalyst to operate (for clarity, the* OsO_4 *is depicted only in the Transition State Complex (TSC) above). This appears to only occur if* ***21*** *flexes rapidly about a structure that complements the optimum transition state of the reaction,* ***23****. The optimum transition state may potentially be formed during the bite opening or the bite closing motion. It is shown here only for the bite opening motion.*

establish, unambiguously, whether a kinematic manufacturing action is present or not, or whether it is dominant or not. It is, nevertheless, likely that at least some, if not a substantial proportion, of the published examples of supramolecular catalysis, may employ such an action, at least in partial measure.

A likely illustrative example in this respect is a bis-cinchona alkaloid catalyst that facilitated the enantioselective dihydroxylation of olefins inside a chiral, bowl-shaped active site within which OsO_4 was complexed [54]. Figure 6 illustrates the probable reaction sequence showing the dihydroxylation of the allyl-4-methoxybenzoate substrate **22** in 98% ee by bis(cinchona) catalyst **21**. The bowl-shaped active site of **21** was built around a pyridazine linker that, as in previous examples, likely constrained conformational flexing of the bowl to a single- or near-single degree of freedom.

A potentially important finding of this work was that the catalyst displayed Michaelis-Menten kinetics. As a result, it was possible to determine the catalyst-reactant binding strength ($1/K_M$) and the catalytic rate at saturation (V_{max}). These proved to be useful quantities in that a positive correlation existed between the extent of overall catalyst–substrate binding ($1/K_M$) and the enantioselectivity of the process [54]. That is, the more binding contacts made between the catalyst and the substrate, the more selective was the reaction. The substrate likely bound to the catalyst active site by the formation of π-contacts between both faces of the allyl and the 4-methoxybenzoate moieties of the two catalyst methoxyquinoline units [54]. Edge contacts may also have been made with the pyridazine ring and with the Os(VIII) moiety [54]. In common with the earlier described examples, contact interactions of this type are highly dynamic, forming and releasing rapidly.

A correlation also existed between the catalytic rate at saturation (V_{max}) and the extent of enantioselectivity. That meant that the faster the overall catalytic rate, the greater the enantioselectivity that was achieved [54]. Kinematic manufacturing machines display a similar property; they tend to work most efficiently when operating at high speed.

The fact that only 98% ee was obtained, rather than 100%, indicates that there was a little less than a 100% likelihood of synchronicity in the necessary, directionally-specific binding of allyl **22** at the key point in each cycle when **21** flexed through a structure that complemented the optimum transition state for the enantioselective reaction. As such, **21** was not a perfect kinematic molecular machine, which would, under normal circumstances, have produced 100% ee. Many enzymes, for example, display perfect (100%) enantioselectivity in their catalyses.

While the precise mechanism of action has not been elucidated in detail, several of the other distinctive features of kinematic manufacturing were also present. For example, the shape of the **21**-OsO_4 active site seems to have structurally complemented the transition state of the reaction during flexing. Thus, even relatively minor changes to the structure of the catalyst destroyed its activity and selectivity, either completely or non-linearly [54].

Moreover, annulated aromatic and heteroaromatic groups, which are generally considered to be inactive as catalytic species in their own right, were clearly utilized in **21** to create a notable catalytic effect.

The catalytic effect in **21** furthermore appears to have depended on every part of the system functioning cooperatively with every other part. That is, the system likely displayed a level of "*functional convergence"*, resulting in a high overall synergy. This seems confirmed by the very substantial enantioselectivity achieved.

The above are all also characteristics of macro-scale industrial kinematic manufacturing machines. It can be concluded that a kinematic manufacturing action likely dominated the catalytic transformation of **22** by **21**.

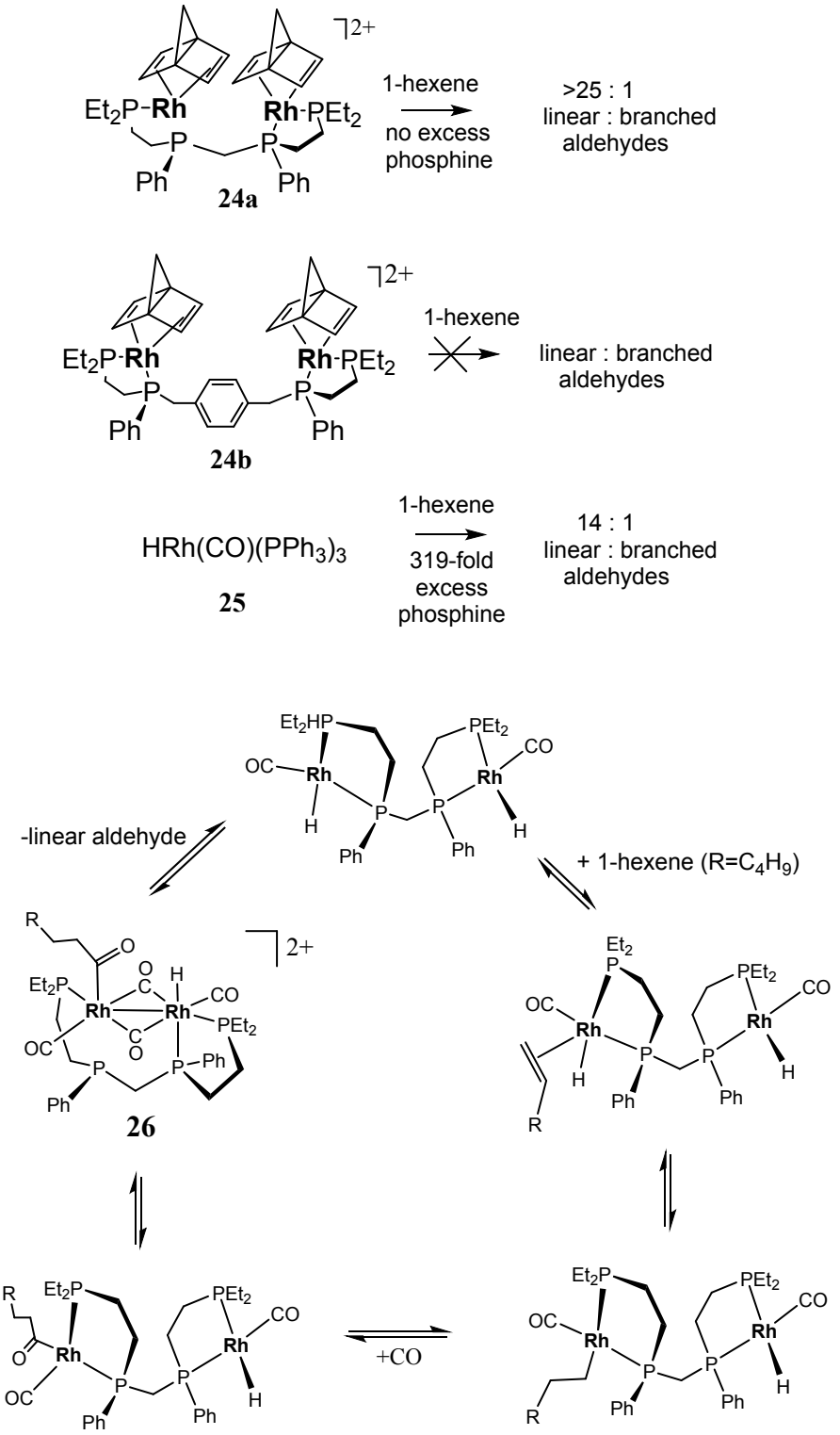

Scheme 12. *Di-rhodium-phosphine hydroformylation catalysts.*

6.2 Organometallic di-Rhodium Catalysts

A range of binuclear catalysts that display cooperativity have been discovered and reviewed, but the role of molecular motion in their actions has not been investigated [55]. One set of examples in this

respect are di-rhodium hydroformylation catalysts like **24a** (Scheme 12) [56], which was discovered by Stanley and co-workers to convert 1-hexene to a >25:1 mixture of linear : branched aldehydes without excess phosphine and at a turnover frequency of 390 h^{-1} Rh^{-1} (under 60 psi pressure at 80 ^{o}C) [56]. By contrast, the analogous *p*-xylene-bridged system **24b**, in which Rh-Rh approach is hindered, is inactive as a catalyst of the same reaction, as is the comparable monomeric catalyst **25** under the same conditions. Monomer **25**, in fact, requires an enormous 319-fold excess of PPh_3 to achieve a notable effect, and then only yields a 14 : 1 ratio of linear : branched aldehydes under the same circumstances [56].

Catalyst **24a** should, in fact, be a much slower catalyst than **25** because of the more basic nature of its tetraphosphine ligand. The rate enhancement was therefore undoubtedly due to a cooperative bimetallic effect involving the two Rh centers.

Later work indicated that the catalytic cycle, in fact, involved a Rh(II) dimer species **26** that formed a Rh-Rh bond during the catalytic process, according to the mechanism depicted at the bottom of Scheme 12 [57]. By constraining the two metal centres to come into close proximity to each other during conformational flexing, it appears that the metals were able to stabilize each other electronically, thereby forming **26** and yielding the regioselective catalytic effect. The fact that the corresponding monomers did not, effectively, display a catalytic effect under comparable conditions, even though there would, presumably, have been no impediment to them forming such a bimetallic intermediate, indicates a requirement for synchronisation in the mechanism. The synchronisation most likely involved the simultaneous presence of a bound hexyl-reactant on one of the Rh centers at the point where conformational flexing facilitated the formation of the Rh^{II}-Rh^{II} bond in **26**. That is, it appears that conformational flexing constrained to a low degree of freedom likely led to the catalytic effect.

Similar effects were provided by the dirhodium catalyst **28a** (Scheme 13), which displayed a 6,800-fold

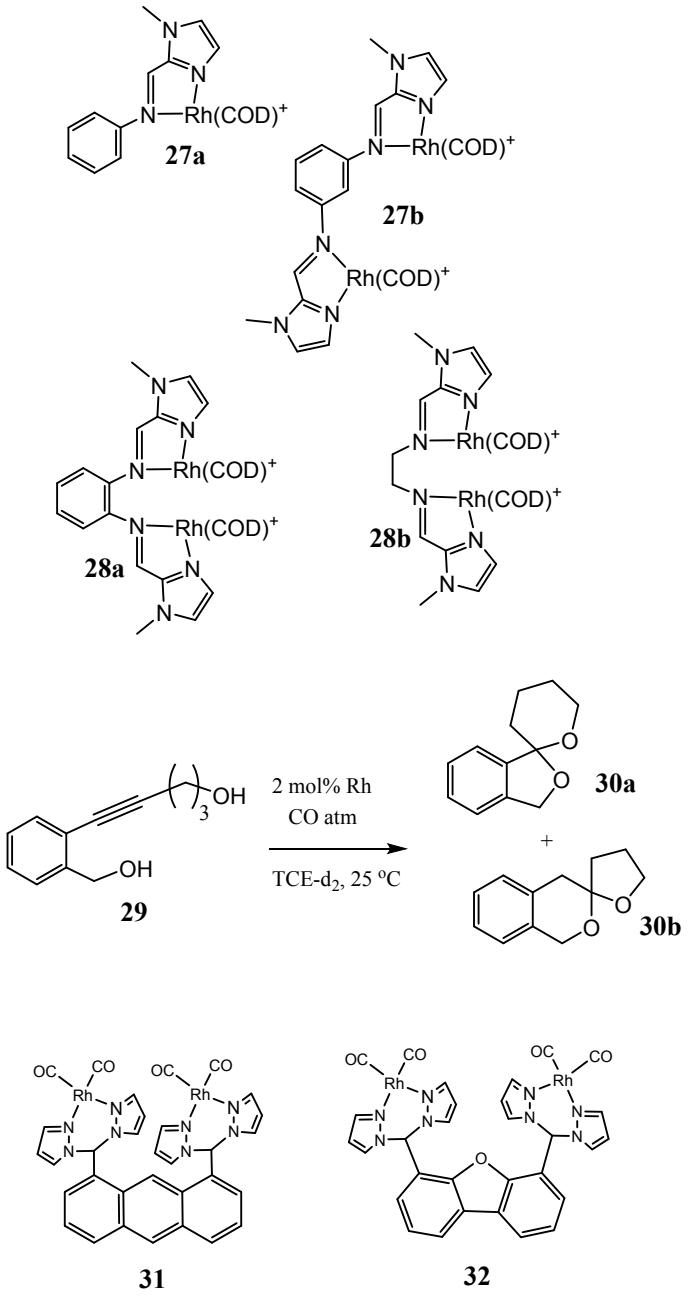

Scheme 13. *Di-rhodium hydroalkoxylation catalysts. (Reproduced and adapted with permission from reference [59])*

amplification in rate compared to its corresponding monomer **27a** in the hydroalkoxylation of the alkynediol **29** to the spiro-ketals **30a-b** (Scheme 13) [58]. Through a comparison with the very much lower efficiency of other bimetallic catalysts, like **27b** and **28b**, the authors concluded that the origin of the large rate amplification lay in the lesser conformational freedom and resulting smaller average intermetallic distance, arising from the use of the *o*-phenylene linker in **28a** [58].

In a later study, linkers of widely varying rigidity were studied for a series of related bis(pyrazol-1-yl) di-rhodium catalysts [59]. The most rigid annulated aromatic linkers afforded the most

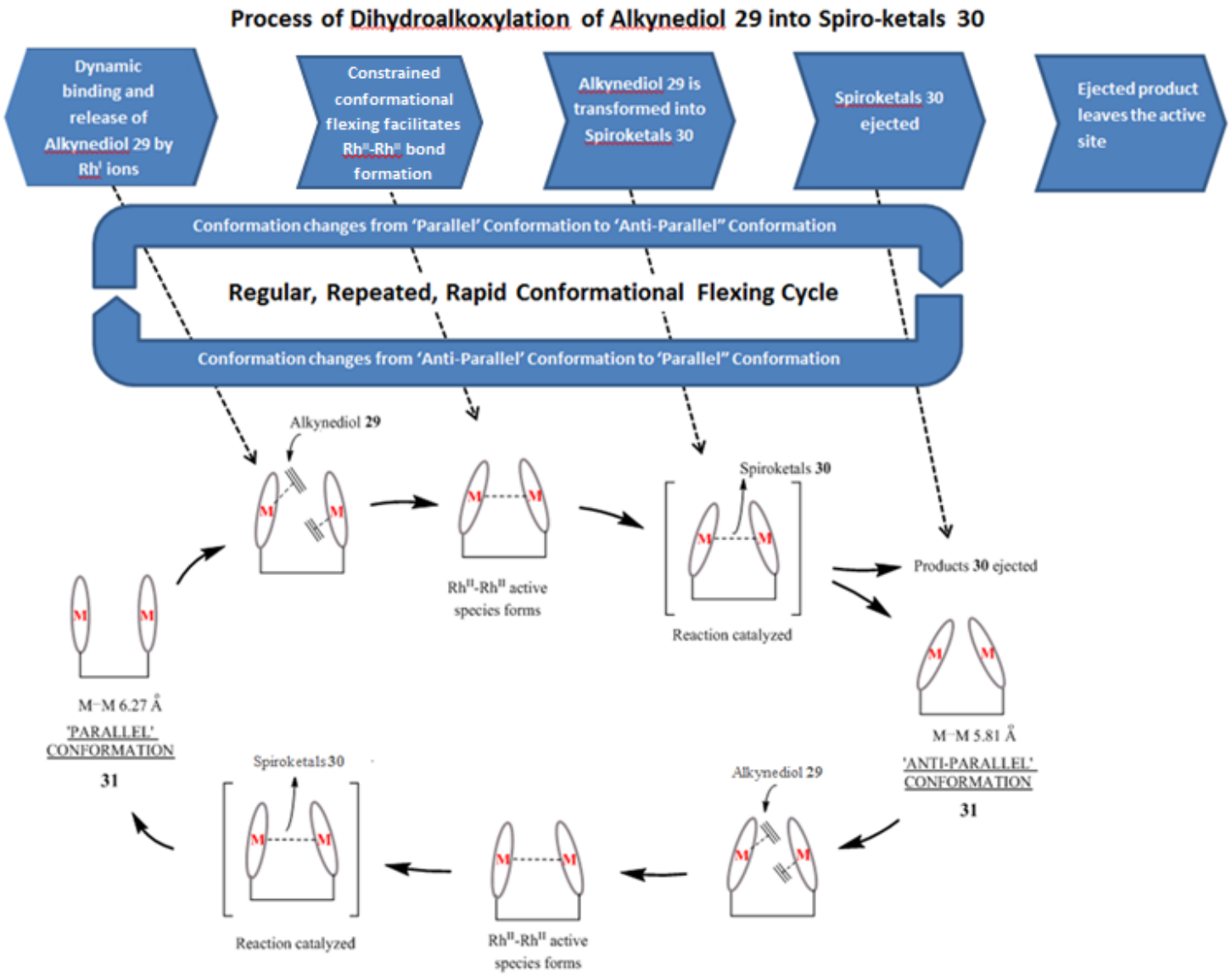

Figure 7. *Schematic of the likely repetitive kinematic cycle for dihydroxylation of alkynediol* ***29*** *during conformational flexing by bis(pyrazol-1-yl) catalyst* ***31*** *(M=Rh^{I}) based on the conformational study in ref. 59. The catalyst* ***31*** *flexes regularly and repeatedly between a 'Parallel' Conformation (Rh-Rh distance 6.27 Å) and an 'Anti-Parallel' conformation (Rh-Rh distance 5.81 Å). During this flexing, a catalytically active intermediate (likely to be a Rh^{II}-Rh^{II} species of the type identified by Stanley et al in ref. [57]) forms, which selectively catalyzes the reaction. It is not known at what point in the flexing cycle the active intermediate forms. The upper pathway indicates the intermediate to be close to the 'Anti-Parallel' structure; the lower pathway shows it close to the 'Parallel' structure.*

active catalysts for transformation of **29** into **30a-b**, with the xanthene linker in **31** providing the greatest rate acceleration. The benzofuran linker in **32** also produced high activity [59].

It should be noted that the xanthene linker in **31** is identical to that of the di-cobalt porphyrin in **4** (Scheme 3), which was earlier noted to utilize a kinematic mode of action in the 4-electron reduction of O_2 to H_2O. The same is true for the benzofuran linker in **32**, which was also present in di-Co porphyrin **7** (Scheme 6). As noted previously, rigid aromatic linkers of this type, which enforce an eclipsed arrangement in a bimetallic system, may have the effect of limiting conformational flexing to a low or single degree of freedom. If that degree of freedom represents or participates in a kinematic manufacturing action, then a new catalytic effect may be created. While the precise mechanism of action of **28a**, **31**, and **32** are not yet established, they may display a similar feature.

The conformational motion of **31**, **32**, and other comparable species was examined in some detail in order to test the hypothesis that the Rh-Rh distance was the critical feature of the cayalysis [59]. Catalyst **31** oscillated between a '*Parallel*' (Rh-Rh distance 6.27 Å) and an '*Anti-Parallel*' (Rh-Rh distance 5.81 Å) conformer at the operating temperature of the catalysis. Catalyst **32**, in fact, displayed the shortest possible Rh-Rh separation during its conformational flexing, which varied between 3.53 and 4.95 Å, depending on the DFT functional used. Regardless of which DFT functional was used, the overall trend in minimum Rh-Rh separation was **32** < **31**. Given that **31** was more active than **32**, it was clear that the catalytic effect did not depend merely on the Rh-Rh distance, but rather on the nature and the rapidity of the flexing.

Figure 7 schematically depicts a possible process for the catalysis, based on the conformational study that was undertaken [59]. The blocks at the top of the figure show the steps followed by the alkynediol **29** in its transformation to the spiroketals **30a-b**. Immediately below that, in the middle of the figure,

the flexing cycle of the catalyst **31**, from the "*Parallel*" to the "*Anti-Parallel*" conformation is shown schematically. At the bottom of the figure is a schematic illustrating the flexing cycle and how **29** may interact with it to form **30a-b**.

As can be seen in Figure 7, during conformational flexing the Rh centers conceivably approach one another until, at an optimum point, a Rh^{II}-Rh^{II} species of the type proposed by Stanley and co-workers [57], likely forms, thereby catalyzing the reaction of **29** into **30a-b**. It is possible that turnovers may occur at both Rh centers during the period that the Rh-Rh dimer existed. It is not known at what point in the flexing cycle the Rh dimer intermediate forms, nor the exact nature of the intermediate. However, synchronicity in the formation of the intermediate and the binding of **29** seems to be required since comparable monomeric Rh^{I} species catalyze the reaction substantially more slowly, by several orders of magnitude, under comparable conditions.

The fact that the equivalent monomeric Rh^{I} species catalyze the reaction at all indicates that the requirement for synchronicity is less pressing in this catalytic system than in the previous examples discussed. This may be because the key intermediate is longer lived than those in the previous examples. Alternatively, it may indicate that binding of the intermediate by the reactant substrate **29** may be stronger and less dynamic than in previously discussed cases. Either way, it is clear that, while a kinematic mode of action is likely present in this system, it is less finely-tuned and truly machine-like than that in Stanley's hydroformylation catalyst **24a** (Scheme 12), whose monomer **25** was inactive under comparable conditions.

Several other binuclear rhodium complexes that catalyze hydroformylation have been reported [60]. Dirhodium carboxylates also catalyze certain carbenoid reactions with Michaelis-Menten kinetics, however virtually no mechanistic information has been provided in those cases [61].

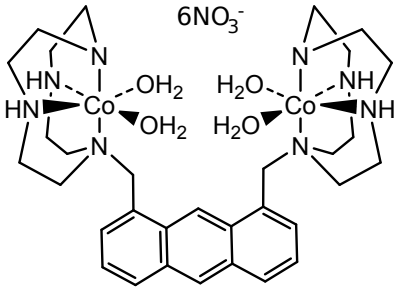

Scheme 14. *Di-cobalt catalyst for hydrolytic cleavage of phosphate esters*

6.3 Phosphate Ester Hydrolysis Catalysts

In 1993, Vance and Czarnik demonstrated efficient hydrolytic cleavage of phosphate esters by the di-cobalt complex **33** (Scheme 14) [62]. Rate accelarations of 10-fold over the equivalent monomers and 10^6- fold over the uncatalyzed reaction were measured. The activity was ascribed to "functional group convergence" arising from the fact that the proximity of the Co ions was strictly controlled, as well as to avoidance of the formation of a non-functional μ-oxo-dimer. A dinuclear copper complex of similar structure was later discovered [63].

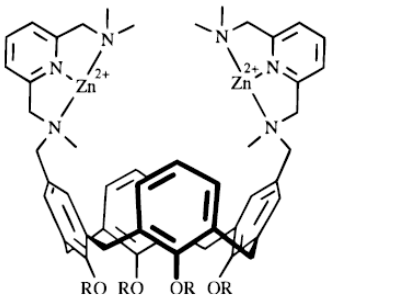

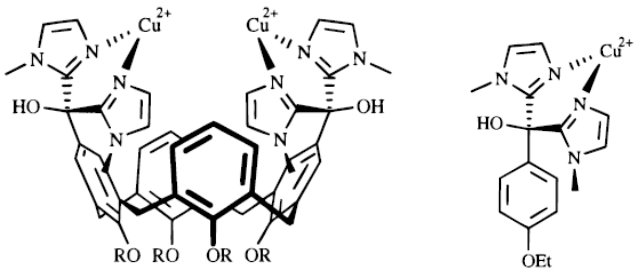

Scheme 15. *Calix[4]arene catalyst for hydrolysis of phosphate esters. (Reproduced with permission from reference [65]).*

Since that time, a range of other dinuclear Co, Zn, and Cu catalysts of this type have been reported to display sometimes remarkable accelerations in rate. Numerous works have reviewed this field [64].

A feature that is common to some of the catalysts that have been discovered, and that appears to be related to the rate enhancements, is constrained conformational motion along a single or low degree of freedom, within an arrangement where the metals appear to effectively eclipse each other.

For example, in a study by Engbert, Rheinhoudt and colleagues [65], it was noted that when the two metal centers in such species were linked by flexible molecular scaffolds they showed negligible rate accelerations in catalytic phosphate ester cleavage. On the other hand, attempts to utilize rigid molecular scaffolds that oriented the metal centers in such a way that the metal-metal distance matched that required for substrate binding, generally resulted in poor binding and activation with accompanying low catalytic turnover. The authors of the study suggested that "a lack of a certain flexibility can give rise to insufficient capacity to bind dynamically the substrate as well as the transition state, which is of crucial importance for catalysis" [65]. In an attempt to remedy these issues, calix[4]arenes appended with two metal ions, were examined as linkers between the two metals.

The calix[4]arene-based dinuclear Zn(II) complex **34** (Scheme 15) proved to be an efficient catalyst for the intramolecular transesterification of an RNA model substrate, namely, 2-hydroxypropyl-nitrophenyl phosphate [65]. Not only was it a catalyst, but it displayed a dramatic rate acceleration of 23,000-fold relative to the equivalent uncatalyzed reaction. The dicopper complex **35**, which contained chelating bisimidazolyl groups that mimic the natural histidine residues**,** displayed a similar rate ampification of 10,000-fold for the same reaction.

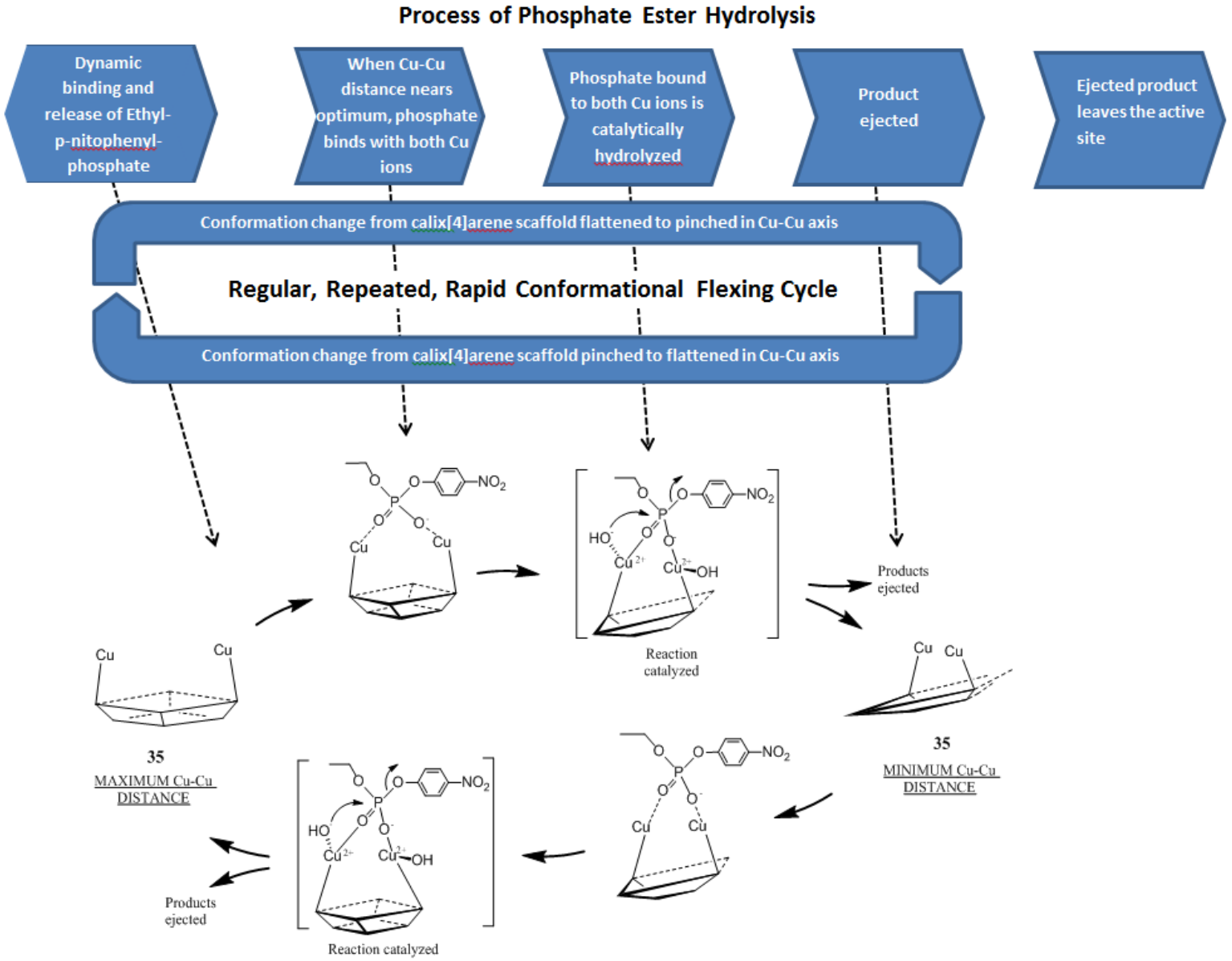

Figure 8. *Schematic of the likely repetitive kinematic cycle for catalytic hydrolysis of ethyl-p-nitrophenyl phosphate during sequential flattening and pinching of the calix[4]arene scaffold in bis-imidazolyl di-copper* ***35****. The catalyst* ***35*** *flexes regularly and repeatedly between a structure in which the calix[4]arene is, first, flattened in the Cu-Cu axis('Maximum Cu-Cu Distance') and then pinched in the Cu-Cu axis ('Minimum Cu-Cu Distance'). The catalytic rate is drastically accelerated relative to the control monomeric Cu species by synchronicity in di-Cu binding by the phosphate during conformational motion through a structure that complements the optimum transition state for the reaction. Catalysis may potentially occur in both the forward and the reverse cycle of the flexing. The metals need to be maintained in an eclipsed configuration at all times.*

In the hydrolysis of a DNA model (ethyl-*p*-nitrophenyl phosphate), catalyst **35** exhibited a rate enhancement of 27,000-fold. By contrast, the equivalent mononuclear catalyst **36** displayed a very much lower catalytic rate (one-fiftieth), indicating that the effect was due to a cooperative interaction between the two metals.

The authors ascribed the above rate amplifications to the ability of the calix[4]arene scaffold to "breathe" – that is, to dynamically adopt flattened/pinched conformations by the simultaneous movement of the two facial aromatic units toward and away from each other [65]. During such "breathing", the appended metal ions must necessarily oscillate regularly, repeatedly, and rapidly toward and away from each other, along a single degree of freedom. The high catalytic efficiency was therefore said to arise from the dynamic binding of the substrate and the "pre-transition state", which was made possible by "rapid, low energy conformational changes of the flexible calix[4]arene backbone". Later work indicated that an eclipsed arrangement of the metals was optimum [66].

Figure 8 schematically depicts the likely catalytic process facilitated by **35**. The uppermost blocks show the steps undertaken by the phosphate substrate during the catalysis. The cycle below and the schematic at the bottom of the figure show the parallel process of flexing by **35** and how it interacts with the phosphate ester in its transformation.

As can be seen in Figure 8, the catalyst likely flexes through structures that, first, complement (and facilitate) di-Cu binding by the phosphate and, then, secondly, complement (and faciltate) the transition state for the hydrolysis reaction. This property of the catalyst appears to enable synchronous phosphate binding and reaction. While the extent of the synchronicity has not been examined in detail, it seems to be required in order to achieve the large rate accelerations. This appears confirmed by the fact that the comparable monomeric Cu species are substantially less active under comparable conditions.

The products were thereafter ejected during further flexing. As mentioned above, the metals need to be maintained in an eclipsed arrangement at all times during the flexing process, in order to achieve optimum activity.

As noted in the previous example, the fact that the equivalent monomers of **35** are catalytically active at all in the reaction, indicates that the requirement for synchronicity in catalyst flexing and substrate binding is less demanding in this system than in previous ones discussed. That is, the system not entirely dependent on the motion of the catalyst and therefore less machine-like in its mode of action.

Nevertheless, **35** displayed Michaelis-Menten kinetics in the above cycle, indicating that its kinetics was determined by a catalyst-substrate complex [65]. The Michaelis complex was said to involve the bound phosphate group doubly Lewis acid activated by coordination of the two Cu(II) ions. A Cu-bound hydroxide ion could then act as a base in the intramolecular transesterification in the case of the RNA model, or as a nucleophile for the DNA model. The remarkably low p*K*a of the Cu(II) bound water molecules in the hydrophobic calix[4]arene **35** was said to mimic the low p*K*a of metal bound water molecules in hydrophobic enzyme active sites.

6.4 Other Catalysts

A wide variety of other homo- and hetereo-bimetallic homogeneous catalysts utilize cooperativity, to greater or lesser extents, in their mode of action [55]. Many of these may conceivably be said to harness machine-like actions, however studies of the role of molecular motion in accelerating (or creating) catalytic rates have been notably absent. For example, while extensive work has been carried out to measure the average metal-metal separation and determine the catalytic optimum in this respect [55(a)], virtually no work has been undertaken to elucidate how the molecular motion involved in these averages affects the catalytic rate or selectivity.

While it is beyond the scope of this review to describe each of the systems and the incomplete work that has been done to date, we list some of the more promising catalysts that may, to a greater or lesser extent, utilize a machine-like action.

A range of cooperative bimetallic olefin polymerization catalysts have been described with modes of action that are likely strongly machine-like [67]. Because of the complexities of their mechanisms it is, unfortunately, not a simple matter to separate and analyse the specific role of molecular motion in the catalytic process. However, molecular motion clearly does play a major role.

Another set of catalysts with interesting and potentially promising machine-like characteristics involve self-assembling porphyrin ligands bearing metal ions such as Zn(II), Cu(I), and Al(III) [68]. Certain of these systems are "switchable" and "lockable". In this respect, they also display machine-like properties, although not of the type that are the subject of the present review.

Jones and James have recently also proposed a "cooperativity catalytic index" to evaluate the cooperative effect in bi- or poly-metallic catalysts of organic transformations [69]. It should be noted however, that this index is limited by the fact that it is based only on kinetic data that assumes the reaction to be first-order in a catalyst.

Bimetallic catalysts that are *not* significantly machine-like in their action should also be mentioned here. Examples of these include, most particularly, various tethered Schiff base catalysts that display catalytic properties that are the same or similar to their equivalent monomers at the same concentration in solution [70]. In these species only a relatively minor cooperative effect exists thanks, typically, to the involvement of a stable, long-lived intermediate whose formation and conversion into a product molecule, does not rely on the molecular motion of the catalyst. For example, various tethered

bimetallic Co epoxidation catalysts display catalytic rates that are not orders of magnitude different to their equivalent monomers at the same concentration [70]. Further discussion in this respect is provided below in section 7.2, Intermolecular Catalysts (*vide infra*).

7. Abiological Catalysts with Noteworthy Properties that are Consistent with a Kinematic Molecular Manufacturing Action

This section reviews species whose catalytic properties can be considered to be remarkable and consistent with, or prospectively indicative of a kinematic manufacturing action, but whose catalytic mechanism has not been elucidated in any detail. Such species may potentially utilize such an action. Most of the examples in this section are based on catalysts discussed in previous sections that employ a kinematic action.

7.1 Intermolecular Catalysts

As noted in section 5.1, many monomeric metalloporphyrins or phthalocyanines catalyze the 2-electron reduction of O_2 into H_2O_2 when adsorbed onto graphite, whereas their dimeric, cofacial analogues facilitate 4-electron reduction, involving O-O bond cleavage, to H_2O under the same circumstances.

An intriguing observation, however, has been that some monomeric metalloporphyrins facilitate the former reaction when adsorbed at low concentrations on graphite, but catalyze the latter reaction when adsorbed at higher concentrations [71]. This has led to suggestions that certain of these species may be effectively adsorbed in a side-on, pairwise arrangement or become adventitiously eclipsed and thereby capable of intermolecular catalysis at higher loadings [71].

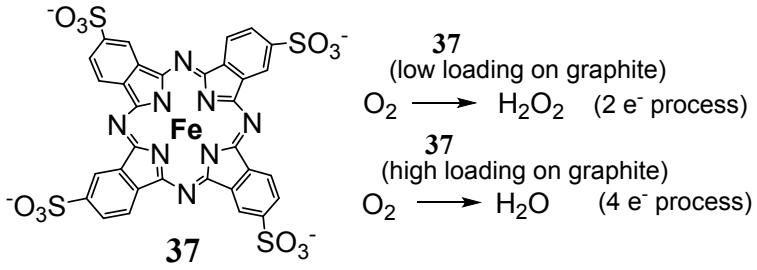

Scheme 16. *Proposed intermolecular oxygen reduction catalysts.*

A pertinent example is the tetrasulfonated iron phthalocyanine **37** (Scheme 16). When adsorbed at low concentrations on graphite, **37** facilitates the electrocatalytic reduction of dioxygen by a 2-electron process giving H_2O_2. As the concentration of **37** is increased however, this rapidly gives way to 4-electron reduction to H_2O [71-73]. The practical difficulty of establishing the mechanism of reaction has made it difficult to determine exactly how this system operates. However, the variation in product as a function of loading is consistent with a cooperative effect. It should be noted here too that some supported metalloporphyrin and phthalocyanine catalysts retain their catalytic properties and, indeed, improve their durability, even after heat treatment to 800 – 1000 ^{o}C and despite the resulting destruction of the organic ligands [71]. This fascinating observation adds another level of complexity to the situation. Such systems are extremely rare examples of "molecular" systems that display the same catalytic properties as their structurally analogous heterogeneous catalysts.

Instead of concentrating a monomeric metalloporphyrin at the surface of an electrode in the hope of favoring a cooperative bimolecular action, it is, alternatively, possible to concentrate it within a conducting matrix, such as within a densely-packed conducting polymer. In some cases, high concentrations of monomeric metalloporphyrins lead to a change in the products generated.

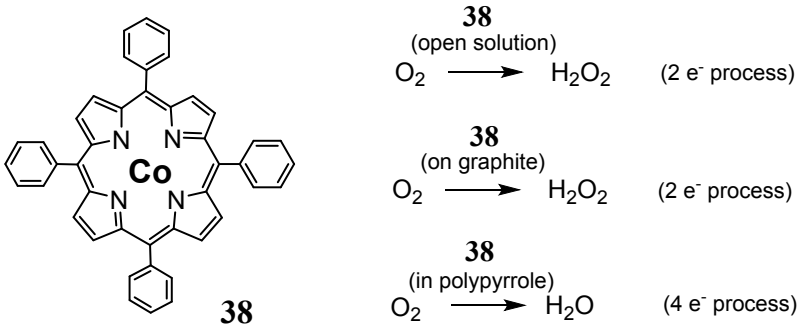

Scheme 17. *Intermolecular oxygen reduction catalysts.*

An example in this respect is Co tetraphenylporphyrin **38** (Scheme 17) [74]. In open solution, **38** catalyzes exclusively the 2-electron reduction of O_2 into H_2O_2. When adsorbed onto graphite, even at high loadings, **38** also facilitates overwhelmingly the 2-electron reduction reaction. However, when incorporated into a densely packed layer of polypyrrole deposited using the vapour-phase polymerization technique, it facilitated predominantly 4-electron reduction to H_2O. Moreover, the proportion of the 4-electron product increased, reaching close to 100%, as the loading of **38** in the polypyrrole was increased. Polypyrrole alone does not catalyze O_2 reduction.

These results were consistent with a statistically significant proportion of the neutral Co-tetraphenylporphyrin **38** being adventitiously disposed within the polypyrrole for a coordinated bi-molecular interaction that favours 4-electron reduction of O_2, yielding H_2O. That proportion may have increased upon concentration of **38** within the polypyrrole [74]. These conclusions were supported by the voltammograms obtained, which were characteristic of microarray electrodes, in which a few highly active H_2O-generating electrocatalytic sites were surrounded by a sea of less active H_2O_2-generating sites [74].

Figure 9 depicts a kinematic process that may possibly operate in this case. The blocks at the top of the figure show the steps followed by the O-atoms, starting with O_2 and ending in H_2O. The cycle below that, and the schematic at the bottom of Figure 9 depicts the regular, repeated molecular motion that could occur in parallel to facilitate the catalysis. In this case, two monomeric Co porphyrins trapped

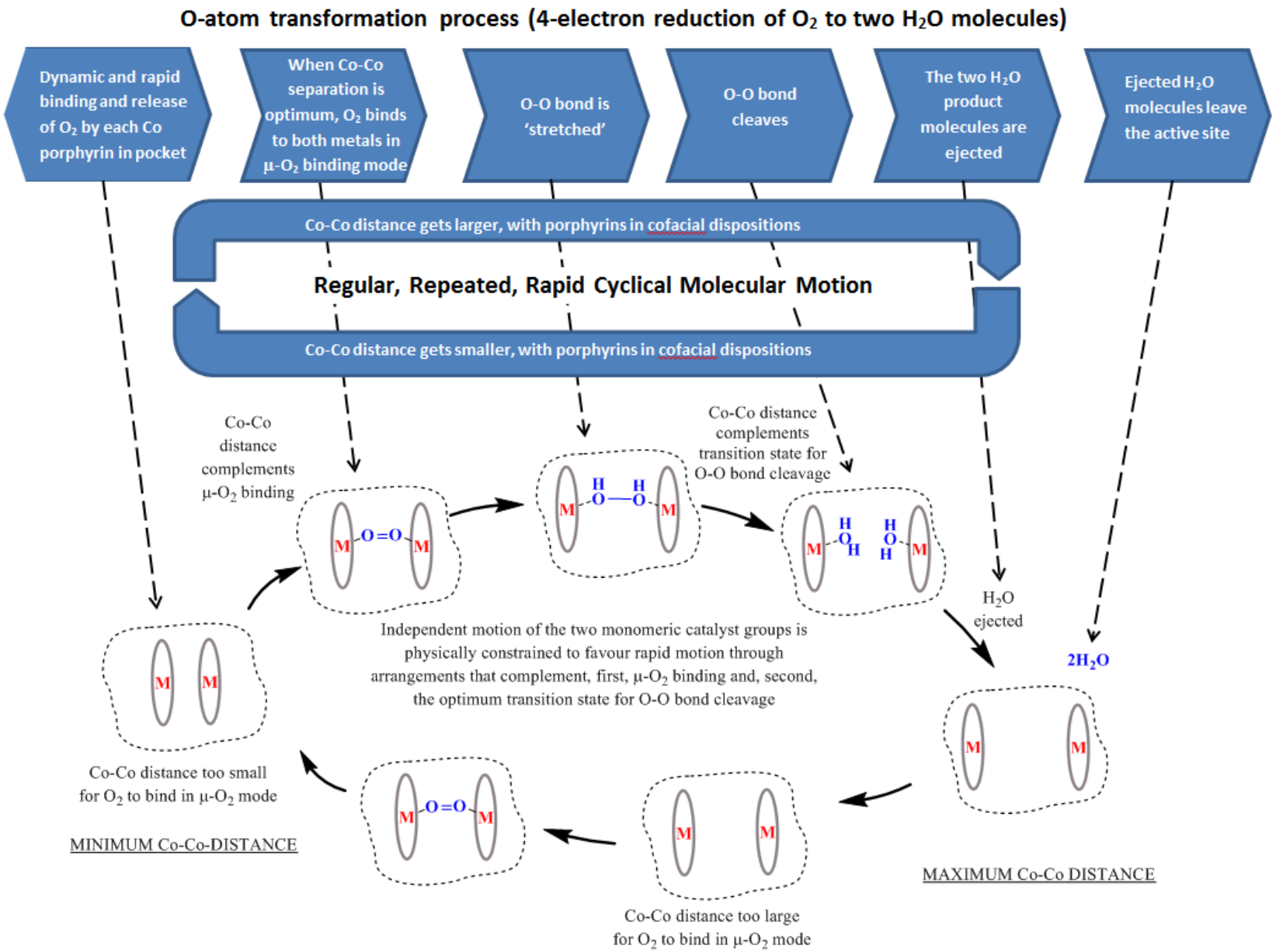

Figure 9. *Schematic of a possible repetitive kinematic cycle for 4-electron reduction of O_2 into H_2O by monomeric porphyrins(M=Co) trapped in a cavity within a thin layer of polypyrrole. The cavity, which is depicted by the dotted line in the Figure, constrains the independent motion of the two Co porphyrin monomers to favour synchronicity in: (i) transient μ-O_2 binding and (ii) a progressive increase in Co-Co separation, that allows the catalyst to operate successfully. This putative mechanism is similar to that of cofacial diporphyrin* ***1*** *(Scheme 1), where two Co porphyrins are constrained by two tethers between them, to achieve a high probability of cofacial dispositions during molecular motion.*

within a cavity in the polypyrrole layer, are constrained during thermal motion, to favour cofacial dispositions, with the Co-Co distance rapidly increasing and decreasing in a cyclical manner. During the resulting process of regular, repetitive molecular motion (not conformational flexing), the Co porphyrin catalytic groups pass sequentially through spatial arrangements that structurally complement, first, O_2 binding (in a μ-O_2 binding mode), and then, secondly, the optimum transition state for O-O bond cleavage. As a result, O_2 binds synchronously to each cofacial Co simultaneously at the moment in the cycle where it is "pulled apart" into two H_2O molecules; that is, at the moment that the molecular motion passes through a structure that complements the optimum transition state of the reaction.

Such a mechanism has a precedent. It would be consistent with the kinematic mechanism that operated for the cofacial Co porphyrin **1** (Scheme 1) described in an earlier section. In **1**, two Co porphyrins were tethered to each other with two flexible connecting chains rather than with a single, rigid linker. The effect of the tethers was to impart upon **1**, a high likelihood of cofacial, eclipsed dispositions during thermal motion, rather than a regular, repeated conformational flexing involving a sequential opening and closing of the co-facial bite angle. As a result thereof, **1** was exclusively a catalyst of 4-electron reduction of O_2 to H_2O. Its equivalent monomer **2** (Scheme 1) by contrast, catalyzed 2-electron reduction to H_2O_2. The process illustrated in Figure 9 therefore effectively, substitutes a high likelihood of proximity and cofacial dispositions arising from molecular tethers (as in **1**) with a high likelihood of proximity and cofacial dispositions arising from physical co-location and trapping.

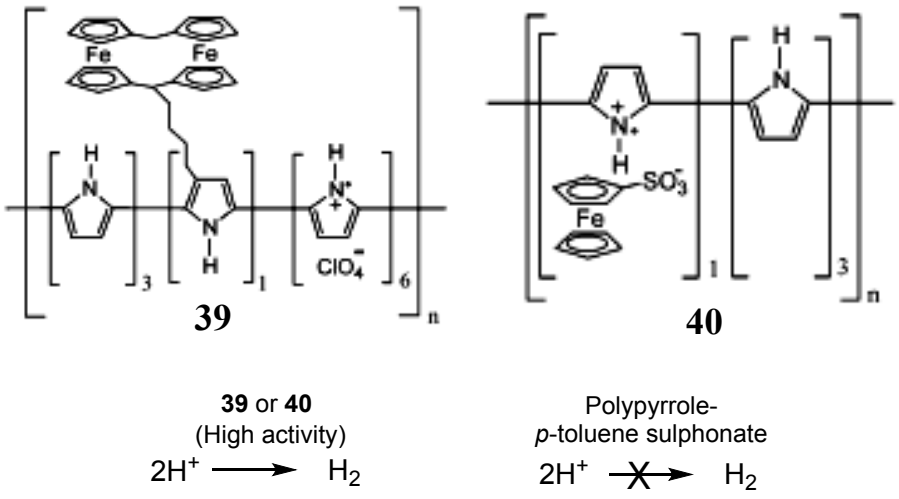

Scheme 18. *Hydrogen-generating catalysts. (Reproduced with permission from reference [75]).*

Another example in similar vein involves the di-ferrocene **15**, which was a kinematic hydrogen generation catalyst (Section 5.2). When **15** was tethered to pyrrole, which was then deposited as conductive polypyrrole **39** (Scheme 18), the resulting electrode was, not unexpectedly, a powerful hydrogen generating catalyst [75]. Less expected however, was the fact that a control coating **40**, containing monomeric ferrocene sulfonate as counter-ion to the polypyrrole, also proved to be a powerful hydrogen generating catalyst [75]. Indeed, **40** was so active that it produced ca. 7-fold more hydrogen than an equivalent platinum surface under comparable conditions. Platinum is widely considered to be the best industrial hydrogen generating catalyst.

The origin of the catalytic activity of **40** appeared to arise from the presence of high loadings of ferrocene sulfonate since a similar coating containing *p*-tolulene sulfonate as counter ion displayed no catalytic effect. Accordingly, it was proposed that a statistically significant proportion of the ferrocene sulfonate had adventitiously been located sufficiently proximate to each other in **40** that it was able to act as in intermolecular catalyst with a cooperative, bimetallic mode of action (much as occurs in **15**). While its catalytic mechanism remains uncertain, due to the practical difficulties of studying the processes present in a porous conducting polymer, **40** certainly produces a remarkable and noteworthy effect. This is precisely what would be expected for a kinematic molecular manufacturing machine.

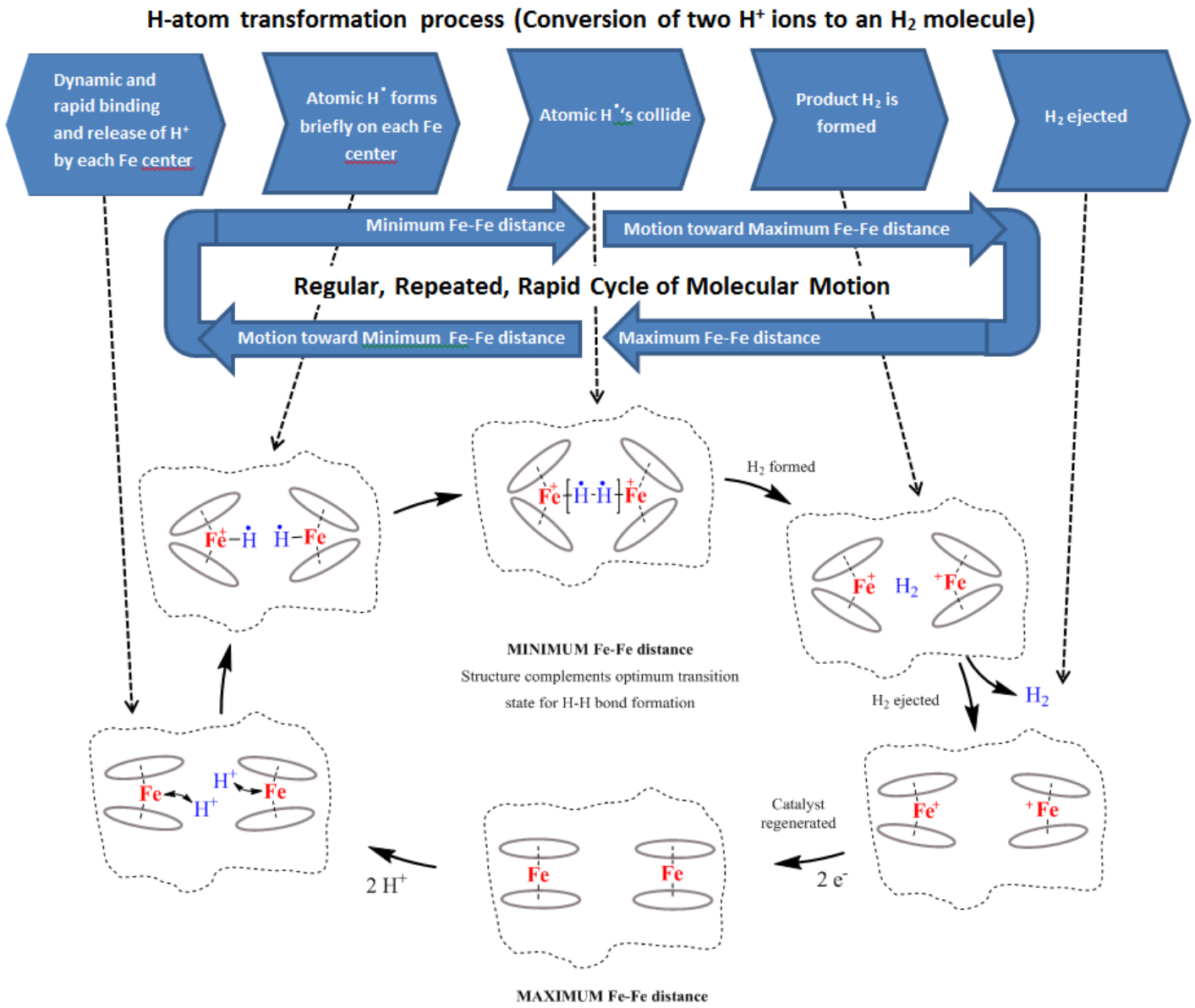

Figure 10. *Schematic of a possible repetitive kinematic cycle for catalytic hydrogen generation by monomeric ferrocenesulphonate dopant trapped in a cavity within a thin layer of polypyrrole. The cavity, which is depicted by the dotted line in the Figure, constrains the independent motion of two ferrocene sulphonate species to favor synchronicity in: (i) transient H^+ binding at each Fe center at the instant that (ii) molecular motion creates a structure that complements the optimum transition state for H-H bond formation. This putative mechanism is similar to that of the [1.1]ferrocenophane* ***15a-c****.*

Figure 10 illustrates a possible kinematic mechanism that could operate in this example. The uppermost blocks in the figure depict the steps that are likely followed by the hydrogen atoms during the process, from H^+ to H_2. Below that is shown the cycle of molecular motion that may conceivably occur in parallel when two ferrocene sulphonate dopants are trapped in close proximity to each within, for example, a cavity in the polypyrrole (outlined by the dotted line in the figure). The schematic at the bottom of the figure depicts how the hydrogen atoms likely interact with the ferrocene sulphonate during the catalysis.

As in the case for **15a** (Figure 5), the two ferrocene Fe centers in Figure 10 would likely each interact dynamically with protons, generating momentary atomic hydrogen species, whose positive charge are delocalized to the attached Fe center. The enforced physical proximity of the monomeric ferrocenes within the polypyrrole layer may then create a high likelihood that two such ferrocenes will bear atomic hydrogen species at the point where they move into an arrangement that complements the optimum transition state for H-H bond formation. H_2 formation would thereafter ensue, with the H_2 product detaching from the two Fe centers during further molecular motion that sees an increase in the Fe-Fe distance.

As in the previous example, the putative mechanism in Figure 10 therefore merely substitutes proximity and constrained motion caused by the presence of two single-carbon tethers between the two ferrocenes of **15a-c** in Figure 5, with proximity and constrained motion caused by enforced physical co-location and trapping of monomeric ferrocene sulfonates in the polypyrrole.

Another extraordinary set of catalysts were based on the di-manganese porphyrin **8** (Scheme 7), which was previously noted to be a catalyst for the oxidation of H_2O to O_2. As noted in section 5.1, the analogous mononuclear manganese porphyrin **9** (Scheme 7) was catalytically inactive for water

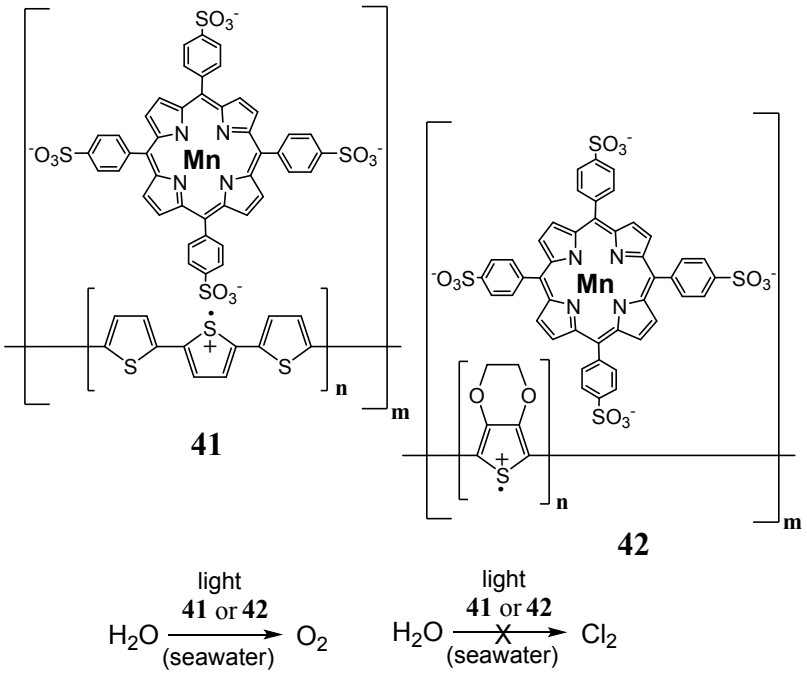

Scheme 19. *Catalysts that are selective for the generation of oxygen, with no chlorine formed, from seawater.*

oxidation. However, when comparable, sulfonated manganese tetraphenyl porphyrin monomers were incorporated within a dense layer of poly(terthiophene) **41** or poly(3,4- ethylenedioxythiophene) (PEDOT) **42**, then the resulting composite was an excellent photocatalyst of water oxidation (Scheme 19) [76,77]. The selectivity of **41** and **42** were such that, even in seawater, they generated only dioxygen O_2, with no chlorine, Cl_2, detected [76,77]. While water oxidation ($2H_2O$ -> $O_2 + 4H^+ + 4e^-$; E^0 1.23 V) is, in theory, thermodynamically favoured over chlorine formation ($2\ Cl^-$ -> $Cl_2 + 2e^-$; E^0 1.36 V) in seawater, the dramatically lower overpotential of chloride oxidation means that chlorine formation dominates under normal circumstances. Indeed, to the best of our knowledge, all other man-made catalysts generate exclusively chlorine when operated in seawater because of its lower overpotential relative to water oxidation (unless immobilized in a cation-exchange resin, in which case a mixture of chlorine and oxygen may be obtained) [78]. The only other catalyst known to be capable to selectively oxidizing water in seawater is the biological catalyst of photosynthesis, the photosystem II water oxidizing complex (PSII-WOC), that is present in marine and hypersaline organisms.

Given that water oxidation catalysts are known to operate by either a bimolecular or monomolecular (nucleophilic attack) mechanism, the observed absence of HClO, which spontaneously equilibrates to form Cl_2 in water, and which should have been formed in the presence of chloride ions, was inferred to indicate a cooperative bimolecular mechanism similar to that in **8** [76]. No physical evidence was available, however, showing catalytic interactions between monomeric porphyrins.

7.2 Intramolecular Catalysts

As noted above, the simplest way in which to overwhelmingly populate a single degree of conformational freedom in a molecule containing two catalytic groups, is to connect the two catalytic groups with a tether. If the tether is short enough and the conformational motion fast enough, a single mode of conformational motion involving rapid, repeated extension and compression of the molecule along the tether, will be created. That is, the catalytic groups will sequentially approach and then retreat from each other along this mode of conformational flexing.

This concept has been investigated by tethering, for example, bi-functional Schiff base catalysts together using an alkyl tether, $-(CH_2)_n-$. In several such cases however, the monomers of the Schiff base catalysts displayed essentially the same catalytic properties as the tethered species [70]. That is, the monomer Schiff bases catalyzed the same reaction at almost the same rate as the tethered di-Schiff bases when the effect of concentration was taken into account [70]. Such behavior is, of course, inconsistent with a kinematic action, since such an action derives, fundamentally, from constrained, rapid, repetitive motion along a single degree of freedom.

The problem in such cases is typically a lack of dynamism in the binding interactions between the reactants and the Schiff base catalytic groups. That is, the substrates bind to the Schiff-base catalytic groups and remain bound to them until catalytic reaction. There is then no need for rapid, repeated

motion to sequester the short-lived, activated forms of the reactants in the formation of new products. Instead, there is no time constraint to product formation, and the securely bound substrates can be transformed without need for rapid motion of the catalyst framework along a single degree of freedom.

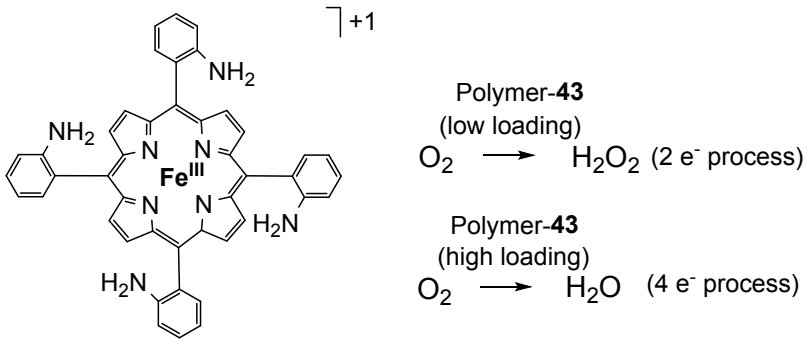

43

Scheme 20. *Macromolecular intramolecular catalysts.*

Some polymers containing multiple tethered catalytic groups do, nevertheless, display novel catalytic properties that are not available to the equivalent, untethered monomeric catalytic groups.

One example in this respect involves a methyl acryl chloride polymer to which iron(III) tetra(*o*-aminophenyl)porphyrin **43** was attached using an amidization reaction (Scheme 20) [79]. The resulting porphyrin-tethered polymer was spin-coated onto a glassy carbon electrode and tested as an oxygen reduction electrocatalyst. When the ratio of poly(methyl acryl chloride) to **43** was such that the surface coverage of **43** was (0.5 – 1.1) x 10^{-9} mol cm^{-2}, 4-electron reduction of O_2 to H_2O occurred in 0.05 M H_2SO_4. However, 2-electron reduction of O_2 to H_2O_2 occurred when the surface coverage was decreased to (1.0 – 1.5) x 10^{-11} mol cm^{-2} [79].

While it is possible that the cumulative increase of appended groups **43** may have altered the electronic and related effects imparted by the polymer on the porphyrins, it is not clear that this would have resulted in a changed catalytic mechanism in this particular case. The polymer should, firstly, have had relatively little electronic influence on the appended metalloporphyrins. Secondly, this should, in any

case, have been much the same at the two different loadings studied, both of which were low compared to the quantity of polymer present.

It is therefore conceivable that in tethering **43** to a reactive monomer that was then polymerized, the regularly repeating nature of the resulting polymer and its flexibility may have populated a mode of flexing that resulted in cooperative, bimolecular catalysis. Beyond the above imputations however, no definitive evidence was reported for such a mode of action.

8. Summary and Conclusions

The mode by which industrial-scale kinematic manufacturing machines operate has been considered. Such machines display several features that are essential to, and highly characteristic of kinematic manufacturing actions. The features include: (1) regular, repetitive and relatively rapid cyclical motion, by (2) components whose actions are coupled, and whose motions are (3) restricted to a single, geometrically-defined degree of freedom, driven by (4) a mechanical impetus, where (5) the manufacturing site interacts dynamically and rapidly to take up starting materials, transform them, and eject the products before the next cycle starts. The coupling of the machine components to each other and their interaction with the starting materials and products, is classically achieved by (6) structural complementarity, which constrains the machine components to move along (7) a single set of optimum, or near-optimum pathways and trajectories. This has the effect of (8) diminishing the total energy consumed in the process and also (9) ensures synchronicity in all of the necessary processes and sub-processes in the manufacturing action. As a result, all working components of the machine are simultaneously coupled to all other working components, creating (10) a synergy that exhibits itself as system-wide cooperativity (also called ‘functional convergence’).

These principles are common to all kinematic manufacturing machines and, when they are simultaneously present, they unequivocally indicate the presence of a machine performing work in a repetitive and sustained fashion. That is, they indicate a kinematic manufacturing process. These principles are not optional, but essential and required for the sustained functioning of the machine. If even one of the above properties is absent or non-optimal in such a machine, it will create an error that compounds non-linearly, leading to the machine not operating properly or not operating at all.

The above principles also apply to molecular catalytic species.

Many of the general properties of enzymes as a class of catalyst are reminiscent of those above. For example, enzymes generally take up and transform their substrates within structures that dynamically interact with and structurally complement the desired target. Moreover, they appear to utilize a set of optimized approach trajectories and pathways facilitated by protein motions that are coupled to each other. As a result, enzymes as a class, typically display the same features of high activity, specificity and reliability that distinguish industrial kinematic manufacturing machines. Just as the sheer productivity of industrial kinematic manufacturing machines inspired awe at the dawn of the industrial age, so does the productive capacity of enzymes at the molecular level today. The kinetics of enzymes at a molecular level can further be said to correspond to those of an industrial manufacturing machine at the macro-level.

While the actions of individual enzymes are typically extremely complex and open to different interpretations, several, more simple man-made catalysts clearly employ kinematic manufacturing actions. For example, cofacial Co diporphyrins tethered in a manner that permits only an eclipsed, repetitive opening and closing of their bite, flex rapidly through structures that complement, first, the optimum mode of O_2 binding and then, secondly, the optimum transition state for O-O bond scission. As a result, these species facilitate μ-O_2 binding immediately before and then at the precise instant that

O-O bond cleavage is strongly favoured. That is, μ-O_2 binding is synchronized with the formation of an optimum pocket for O-O scission, resulting in 4-electron reduction of O_2 to 2 H_2O molecules.

By contrast, their equivalent monomeric Co porphyrins, or equivalent diporphyrins that are not constrained to an eclipsed state during repetitive opening and closing of their bite, do not and can not facilitate O-O bond cleavage. They instead facilitate 2-electron reduction of O_2 to H_2O_2, in which the O-O bond remains intact.

Similarly, tethered di-ferrocenes that flex rapidly about a structure that complements the optimum transition state for H-H bond formation, are powerful, active and selective hydrogen generation catalysts. They generate 5 molecules of hydrogen per second continuously for over 5 days of testing, equating to more than 2.16 million H_2 molecules produced per molecular catalyst, without any de-activation. This extraordinary capability arises because each ferrocene Fe is favoured to simultaneously bear a bound and activated proton at the precise instant that the catalyst forms a pocket that is optimum for H-H bond formation. That is, it derives from synchronicity in the two, independent, dynamic processes of proton binding at the Fe centers and conformational flexing of the di-ferrocene framework. The synchronicity is created by the interplay of rapid conformational flexing about an optimum structure and the dynamic nature of the catalyst-reactant binding interactions.

By contrast, equivalent monomer ferrocenes are entirely inactive as hydrogen generation catalysts. That is, without the presence of a framework that rapidly flexes about an optimum catalytic pocket, monomeric ferrocenes have an exceedingly low likelihood of bringing two bound protons into collision with each other. The same is true for di-ferrence species that: (i) flexed too slowly or (ii) that did not flex about a structure that complemented the target optimum transition state.

Other molecular catalysts employ mechanisms consistent with a kinematic manufacturing action. For example, a bis(cinchona) alkaloid catalyst that is constrained to flex along a low degree of freedom facilitated highly enantiospecific asymmetric dihydroxylation of an allyl. This occurred because the catalyst flexed repetitively through a structure that complemented the optimum transition state of the reaction, with the dynamically-binding allyl simultaneously attached in a directionally-specific arrangement. A correlation existed in this case, between the extent of enatioselectivity and the overall rate of the catalysis; the faster the catalytic rate, the greater the enantioselectivity that was achieved. Kinematic manufacturing machines display a similar property; they tend to work most efficiently when operating at high speed.

Di-rhodium-phosphine hydroformylation catalysts and calix[4]arene-based di-copper phosphate ester hydrolysis catalysts have also been described that harness the elements of regular, reptitive motion through structures that are, firstly, optimum for the uptake of reactant molecules in ideal dispositions and, secondly, immediately thereafter, optimum for catalytic transformation of those reactant molecules. By these means synchronicity was achieved in the necessary features of simultaneous reactant binding and catalyst motion at the critical juncture of bond transformation. Increases in reaction rate by orders-of-magnitude were thereby achieved.

Inter-molecular catalysts may possibly also make use of kinematic manufacturing actions of this type. In such cases, regular, reptitive motion was achieved not by physically tethering elements together, but rather by constraining equivalent monomeric catalytic groups to closely proximate thermal motion within densely packed host matrices.

While the properties and capabilities of industrial kinematic manufacturing machines are well-known, the development of man-made analogues that operate at the molecular scale remains a key challenge in science. A few such systems already exist, albeit only in relatively rudimentary form. In order to

expand these into a larger group, this work has aimed to describe, elaborate upon, and stimulate consideration of kinematic manufacturing processes and how they may manifest themselves in molecular systems.

9. Acknowledgements

DB thanks the Australian Research Council for an Australian Post-Graduate Award (APA). DB thanks the Australian Research Council‘s Centre of Excellence for Electromaterial Science for financial support. GFS and SH thank the Program for Foreign Experts of the Peoples Republic of China for financial support.

Keywords: Machine • kinematic • enzyme • catalysis • molecule • motion

10. References

[1] J. S. Beggs, Kinematics, Taylor & Francis, 1983, p. 1. ISBN 0-89116-355-7.

[2] R.P. Feynman, Engineering and Science 23 (1960) 22.

[3] For example, enzymes have been referred to as "machines" in D. W. Moss, Enzymes, Oliver and Boyd, 1968, p. 70, and references therein.

[4] See for example: (a) K. E. Drexler, Proc. Natl. Acad. Sci. USA Phys. Sci. 78 (1981) 5275; (b) K. Ariga, K. Minami, M. Ebara, J. Nakanishi, Polymer J. 48 (2016) 371; (c) K. Ariga, T. Mori, S. Ishihara, K. Kawakami, J. P. Hill, Chem. Mat. 26 (2014) 519.

[5] (a) K. E. Drexler, Engines of Creation: the Coming Era of Nanotechnology, Anchor-Doubleday, New York, 1986; (b) K. E. Drexler, Nanosystems: Molecular Machinery, Manufacturing and Computation, Wiley, New York, 1992.

[6] See, for example: S. Erbas-Cakmak, D. A. Leigh, C. T. McTernan, A. L. Nussbaumer, Chem. Rev. 115 (2015) 10081 and references therein.

[7] C. S. Vogelsberg, M. A. Garcia-Garibay, Chem. Soc. Rev. 41 (2012) 1892.

[8] G. F. Swiegers (Ed.) Mechanical Catalysis; Methods of Heterogeneous, Homogeneous, and Enzymatic Catalysis. John Wiley and Sons, New York, 2008: (a) Chap 5; (b) Chap 8.

[9] J. Chen, P. Wagner, G. F. Swiegers, Chap 6 in Bioinspiration and Biomimicry in Chemistry, Ed: G. F. Swiegers, Wiley, New York, 2012.

[10] Twenty one distinct hypotheses for enzymatic catalysis were listed in: M. I. Page, Chap 1 in Enzyme Mechanisms, (Eds: M. I. Page, A. Williams), Royal Soc. Chem., 1989, p. 1, and references therein.

[11] 'Lock-and-key' theory: see L. Stryer, Biochemistry, Third Edition, W. H. Freeman and Company, New York, 1988, p. 177-200. For later modifications, see: (a) J. B. S. Haldane, Enzymes, Longmans, Green and Co. 1930, p. 182, and (b) D. E. Koshland, Proc. Natl. Acad. Sci. USA 44 (1958) 98.

[12] L. Pauling, Nature 161 (1948) 707. See also: L. Pauling, Chem. Eng. News 24 (1946) 1375.

[13] This has been supported by subsequent work. See, for example: (a) D. H. Williams, E. Stephens, M. Zhou, Chem. Commun. (2003) 1973, and references therein. (b) Another demonstration of the importance of structural complementarity to the optimum transition state is the fact that even minor modifications to the protein sequence can dramatically diminish enzymatic activity and specificity; see, for example: W. N. Lipscombe, Structural and Functional Aspects of Enzymatic Catalysis (Eds: H. Eggerer, R. Huber), Springer-Verlag, Berlin, 1981, p. 17, and references therein.

[14] See, for example: (a) "Proximity Effect": T. C. Bruice, Ann. Rev. Biochem. 45 (1976) 331, (b) "Near-Attack Conformers": T. C. Bruice, Acc. Chem. Res. 35 (2002) 139, and references therein. See also: (c) T. C. Bruice, F. C. Lightstone, Acc. Chem. Res. 32 (1999) 127; (d) E. Lau, T. C. Bruice, J. Am. Chem. Soc. 122 (2000) 7165; (e) T. C. Bruice, S. J. Benkovic, Biochemistry 39 (2000) 6267.

[15] See, for example: (a) A. Tousignant, J. N. Pelletier, Chem. Biol. 11 (2004) 1037; (b) S. Hammes-Shiffer, Biochem. 41 (2002) 13335; (c) S. Hammes-Schiffer, S. J. Benkovic, Annu. Rev. Biochem. 75 (2006) 519; (d) S. J. Benkovic, S. Hammes-Schiffer, Science 301 (2003) 1196; (e) D. Boehr, D. McElheny, H. J. Dyson, P. E. Wright, Science 313 (2006) 1638; (f) M. Vendruscolo, C. Dobson, Science 313 (2006) 1586.

[16] (a) E. Z. Eisenmesser, D. A. Bosco, M. Akke, D. Kern, Science 295 (2002) 1520; (b) E. Z. Eisenmesser, O. Millet, W. Labeikovsky, D. M. Korzhnev, M. Wolf-Watz, D. A. Bosco, J. J. Skalicky, L. E. Kay, D. Kern, Nature 438 (2005) 117.

[17] R. J. P. Williams, Trends in Biochem. Sci. 18 (1993) 115 and references therein.

[18] G. F. Swiegers, J. Huang, R. Brimblecombe, J. Chen, G. C. Dismukes, U. T. Mueller-Westerhoff, L. Spiccia, G. G. Wallace, Chem. Eur. J. 15 (2009) 4746.

[19] J. P. Collman, M. Marrocco, P. Denisevich, C. Koval, F. C. Anson, J. Electroanal. Chem. Interfac. Electrochem. 101 (1979) 117.

[20] J. P. Collman, P. Denisevich, Y. Konai, M. Marrocco, C. Koval, F. C. Anson, J. Am. Chem. Soc. 102 (1980) 6027.

[21] R. R. J. Durand, C. S. Benscome, J. P. Collmann, F. C. Anson, J. Am. Chem. Soc. 105 (1983) 2710.

[22] (a) J. P. Collman, P. S. Wagenknecht, J. E. Hutchison Angew. Chem. Int. Ed. Engl. 33 (1994) 1537, and references therein, (b) C. K. Chang, H. Y. Abdalmuhdi, J. Am. Chem. Soc. 106 (1984) 2725; (c) Y. Le Mest, M. L'Her, J. P. Collman, N. H. Hendricks, L. McElwee-White, J. Am. Chem. Soc. 108 (1986) 533.

[23] C. J. Chang, Y. Deng, C. Shi, C. K. Chang, F. C. Anson, D. G. Nocera Chem. Commun. (2000) 1355.

[24] (a) J. P. Collman, N. H. Hendricks, K. Kim, C. S. Bencosme, J. Chem. Soc., Chem. Commun. (1987) 1537; (b) H. Y. Liu, I. Abdalmuhdi, C. K. Chang, F. C. Anson, J. Phys. Chem. 89 (1985) 665; (c) J. P. Collman, K. Kim, J. Am. Chem. Soc. 108 (1986) 7847.

[25] Guilard, R.; Lopez, M.-A.; Tabard, A.; Richard, P.; Lecomte, C.; Brandes, S.; Hutchison, J. E.; Collman, J. P. J. Am. Chem. Soc. 114 (1992) 9877.

[26] J. P. Collman, J. E. Hutchison, M.-A. Lopez, A. Tabard, R. Guilard, W. K. Seok, J. Ibers, M. L'Her, J. Am. Chem. Soc. 114 (1992) 9869.

[27] (a) Y. Naruta, M.-A. Sasayama, T. Sasaki, Angew. Chem. Int. Ed. Engl. 33 (1994) 1839; (b) Y. Shimazaki, T. Nagano, H. Takesue, B. Ye, F. Tani, Y. Naruta, J. Inorg. Biochem. 96 (2003) 227; (c) Y. Naruta, M. A. Sasayama, J. Chem. Soc. Chem. Commun. 23 (1994) 2667.

[28] D. Ricard, B. Andrioletti, M. L'Her, B. Boitrel, Chem. Commun. (1999) 1523.

[29] J. P. Collman, L. Fu, P. C. Herrmann, X. Zhang, Science 275 (1997) 949.

[30] J. P. Collman, R. Schwenninger, M. Rapta, M. Bröring, L. Fu, Chem. Commun. (1999) 137.

[31] J. P. Collman, L. Fu, P. C. Herrmann, Z. Wang, M. Rapta, MM. Bröring, R. Schwenninger, B. Boitrel, Angew. Chem. Int. Ed. Engl. 37 (1998) 3397.

[32] J. P. Collman, M. Rapta, M. Bröring, L. Raptova, R. Schwenninger, B. Boitrel, L. Fu, M. L'Her, J. Am. Chem. Soc. 121 (1999) 1387.

[33] J. P. Collman, Inorg. Chem. 36 (1997) 5145.

[34] J. P. Collman, Y. Ha, P. S. Wagenknecht, M.-A. Lopez, R. Guilard, J. Am. Chem. Soc. 115 (1993) 9080.

[35] J. P. Collman, J. E. Hutchinson, P. S. Wagenknecht, N. S. Lewis, M. A. Lopez, R. Guilard, J. Am. Chem. Soc. 112 (1990) 8206.

[36] T. E. Bitterwolf, A. C. Ling, J. Organomet. Chem. 57 (1973) C15.

[37] U. T. Mueller-Westerhoff, T. J. Haas, G. F. Swiegers, T. K. Leipert, J. Organomet. Chem. 472 (1994) 229.

[38] U. T. Mueller-Westerhoff, Angew. Chem. Int. Ed. Engl. 25 (1986) 702 and references therein.

[39] U. T. Mueller-Westerhoff, A. Nazzal, J. Am. Chem. Soc. 106 (1984) 5381.

[40] A. Cassens, P. Eilbracht, A. Nazzal, W. Prössdorf, U. T. Mueller-Westerhoff, J. Am. Chem. Soc. 103 (1981) 6367.

[41] A. Karlsson, A. Broo, P. Ahlberg, Can. J. Chem. 77 (1999) 628.

[42] U. T. Mueller-Westerhoff, G. F. Swiegers, Chem. Lett. (1994) 67.

[43] A. Waleh, G. H. Loew, U. T. Mueller-Westerhoff, Inorg. Chem. 23 (1984) 2859.

[44] U. T. Mueller-Westerhoff, T. J. Haas, G. F. Swiegers, T. K. Leipert, J. Organomet. Chem. 472 (1994) 229.

[45] A. F. Diaz, U. T. Mueller-Westerhoff, A. Nazzal, M. Tanner, J. Organomet. Chem. 236 (1982) C45.

[46] A. L. Rheingold, U. T. Mueller-Westerhoff, G. F. Swiegers, T. J. Haas, Organomet. 11 (1992) 3411.

[47] M. Hillman, S. Michaile, S. W. Feldberg, J. Eisch, Organomet. 4 (1985) 1258.

[48] S. Michaile, M. Hillman, Organomet. 7 (1988) 1059.

[49] G. Rowlands, Tetrahedron 57 (2001) 1865.

[50] M. Shibasaki, H. Sasai, T. Arai, Angew. Chem. Int. Ed. Engl. 36 (1997) 1236.

[51] P. Molenveld, J. F. J. Engbersen, D. N. Reinhoudt, Chem. Soc. Rev. 29 (2000) 75 and references therein.

[52] H. Steinhagen, G. Helmchen, Angew. Chem. Int. Ed. Engl. 35 (1996) 2339.

[53] A. J. Kirby, Angew. Chem. Int. Ed. 35 (1996) 707.

[54] E. J. Corey, M. C. Noe, J. Am. Chem. Soc. 118 (1996) 319.

[55] (a) I. Bratko, M. Gomez, Dalton Trans. 42 (2013) 10664; (b) J. Park, S. Hong, Chem. Soc. Rev. 41 (2012) 6931; (c) D. G. H. Hetterscheid, S. H. Chikkali, B. de Bruin, J. N. H. Reek, ChemCatChem 5 (2013) 2785; (d) N. P. Mankad, Chem. Eur. J. 22 (2016) 5822; (e) J. I. van der Vlugt, Eur. J. Inorg. Chem. (2012) 363.

[56] (a) S. A. Laneman, F. R. Fronczek, G. G. Stanley, J. Am. Chem. Soc. 110 (1988) 5585; (b) S. A. Laneman, G. G. Stanley, in Homogeneous Transition Metal Catalyzed Reactions: Developed from a Symposium; Eds: W. R. Moser, D. W. Slocum, American Chemical Society: Washington, DC, 1992.

[57] (a) S. A. Laneman, G. G. Stanley, Advances in Chemistry Series 230 (1992) 349 (American Chemical Society, Washington DC); (b) R. C. Matthews, D. K. Howell, W.-J. Peng, S. G. Train, W. D. Treleaven, G. G. Stanley, Angew. Chem. Int. Ed. Engl. 35 (1996) 2253.

[58] S. W. S. Choy, M. J. Page, M. Babhade, B. A. Messerle Organomet. 32 (2013) 4726.

[59] M. G. Timerbulatova, M. R. D. Gatus, K. Q. Vuong, M. Bhadbhade, A. G. Algarra, S. A. Macgregor, B. A. Messerle, Organomet. 32 (2013) 5071.

[60] (a) P. Escaffre, A. Thorez, P. J. Kalck, Chem. Soc. Chem. Commun. (1987) 146; (b) J. Jenck, P. Kalck, E. Pinelli, M. Siani, A. Thorez, J. Chem. Soc. Chem. Commun. (1988) 1428.

[61] M. C. Pirrung, H. Liu, A. T. Morehead, J. Am. Chem. Soc. 124 (2002) 1014.

[62] D. H. Vance, A. W. Czarnik, J. Am. Chem. Soc. 115 (1993) 12165.

[63] M. J. Young, J. Chin, J. Am. Chem. Soc. 117 (1995) 10577.

[64] (a) T. Nittymaki, H. Lonnberg, H. Org. Biomol. Chem. 4 (2006) 15; (b) F. Mancin, P. Scrimin, P. Tecilla, U. Tonellato, Chem. Commun. (2005) 2540; (c) J. R. Morrow, O. Iranzo, Curr. Opin. Chem. Biol. 8 (2004) 192; (d) C. Liu, M. Wang, T. Zhang, H. Sun, Coord. Chem. Rev. 248 (2004) 147; (e) J. A. Cowan, Curr. Opin. Chem. Biol. 5 (2001) 634; (f) E. Kimura, Curr. Opin. Chem. Biol. 4 (2000) 207; (g) P. Molenveld, J. F. J. Engbersen, D. N. Reinhoudt, Chem. Soc. Rev. 29 (2000) 75; (h) K. K. Bashkin, Curr. Opin. Chem. Biol. 3 (1999) 752; (i) N. H. Williams, B. Takasaki, M. Wall, J. Chin, Acc. Chem. Res. 32 (1999) 485; (j) E. L. Hegg, J. N. Burstyn, Coord. Chem. Rev. 173 (1998) 133; (k) S. J. Franklin, Curr. Opin. Chem. Biol. 5 (2001) 201; (l) M. Komiyama, J. Sumaoka, J. Curr. Opin. Chem. Biol. 2 (1998) 751.

[65] P. Molenveld, J. F. J. Engbersen, H. Kooijman, A. L. Spek, D. N. Reinhoudt, J. Am. Chem. Soc. 120 (1998) 6726.

[66] R. Cacciapaglia, A. Casnati, L. Mandolini, D. N. Reinhoudt, R. Salvio, A. Sartori, R. Ungaro, J. Am. Chem. Soc. 128 (2006) 12322.

[67] (a) J. P. McInnis, M. Delferro, T. J. Marks, Acc. Chem. Res. 47 (2014) 2545; (b) A. Zecchina, E. Groppo, S. Bordiga, Chem. Eur. J. 13 (2007) 2440.

[68] (a) M. Schmittel, Chem. Commun. (2015) 51, 14956; (b) M. Schmittel, S. De, S. Pramanik, Angew. Chem. Int. Ed. 51 (2012) 3832; (c) R. K. Totten, P. Ryan, B. Kang, S. J. Lee, L. J. Broadbelt, R. Q. Snurr, J. T. Hupp, S. T. Nguyen, Chem. Commun. 48 (2012) 4178.

[69] N. D. Jones, B. R. James, Adv. Synth. Catal. 344 (2002) 1126.

[70] (a) R. G. Konsler, J. Karl, E. N. Jacobsen, J. Am. Chem. Soc. 120 (1998) 10780; (b) E. N. Jacobsen, Acc. Chem. Res. 33 (2000) 412; (c) J. A. Kalow, A. G. Doyle, J. Am. Chem. Soc. 133 (2011) 16001.

[71] P. Vasudevan, Santosh, N. Mann, S. Tyagi, Transition Met. Chem. 15 (1990) 81 and references therein.

[72] S. Zecevic, B. Simic-Glavaski, E. J. Yeager, Electroanal. Chem. 196 (1985) 339.

[73] M. Brezina, W. Khalil, J. Koryta, M. Musilova, J. Electroanal. Chem. 77 (1977) 237.

[74] J. Chen, W. Zhang, D. Officer, G. F. Swiegers, G. G. Wallace, Chem. Commun. (2007) 3353.

[75] J. Chen, J. Huang, G. F. Swiegers, C. O. Too, G. G. Wallace, Chem. Commun. (2004) 308.

[76] J. Chen, P. Wagner, L. Tong, G. G. Wallace, D. L. Officer, G. F. Swiegers, Angew. Chem. Int. Ed. 51 (2012) 1907.

[77] J. Chen, P. Wagner, L. Tong, D. Boskovic, W. Zhang, D. Officer, G. G. Wallace, G. F. Swiegers, Chem. Sci. 4 (2013) 2797.

[78] R. Brimblecombe, J. Chen, P. Wagner, T. Buchhorn, G. C. Dismukes, L. Spiccia, G. F. Swiegers, J.. Mol. Catal. A Chem. 338 (2011) 1.

[79] A. Bettelheim, R. J. H. Chan, T. Kuwana, J. Electroanal. Chem. 99 (1979) 391.